ELECTRICAL PROPERTIES OF JUNCTIONS BETWEEN ALUMINIUM AND POLY(3-(2,5-DIOCTYLPHENYL)-THIOPHENE) (PDOPT)

A Thesis Submitted to the
School of Graduate Studies
Addis Ababa University

In Partial Fulfilment of the
Requirements for the Degree of
Master of Science in Physics

BY

GIRMA GORO

JUNE 1998

ADDIS ABABA

To the memory of

Jitu Wayessa

Acknowledgement

I not only express my deepest gratitude and special affection to my advisor and instructor Dr. Bantikassegn Workalemahu, but also I honour him for his constant assistance, invaluable guidance and stimulating atmosphere he created with out any reservation till the completion of this work. It is a great privilege to work with him.

I would like to express my sincere thanks to my father, mother, brothers and sisters for their encouragement. I thank the Physics Department community and my instructors in the Department for their help in one way or another for my success. I would like to express my heartfelt thanks to Ato Dejene Birru, Ato Teshome Alemayehu, Ato Getachew Anberbir and all my friends for their friendly co-operation in every aspect.

I thank my wife, Metasebia Mekonnen, and our kids Jalle and Hilu for their love and concern. Metasebia, I appreciate your decision to confront loneliness when I was supposed to join this program. I know how difficult it was to be alone to look after two kids. But the Almighty enables you/us. Praise be to God.

Last, but not least, Oromia Education Bureau is acknowledged for sponsoring me to join the School of Graduate Studies.

CONTENTS

List of tables

List of figures

Abstract

This thesis is based on the study of interface properties between a reactive metal and a neutral conjugated polymer. The polymer used is poly(3-(2,5-dioctylphenyl)-thiophene) (PDOPT). The techniques employed are absorption spectroscopy, current-voltage and complex impedance spectroscopy measurements.

The absorption measurement reveals that the polymer, PDOPT, has an energy gap of about 2.02 eV and hence it belongs to the class of semiconducting materials. The I-V characteristic of Al/PDOPT/ITO structure shows symmetrical but non-ohmic curves. The complex impedance analysis exhibits a single semicircle whose diameter depends on the magnitude of the applied voltage. For smaller values of the applied voltage, both for the reverse and forward biases, the extrapolated diameter of the semicircle is larger. This value is consistent with the result of the I-V measurements. So this device, Al/PDOPT/ITO, may be considered as a metal-semiconductor device with no rectifying Schottky barrier formation at the Al/PDOPT interface. The small value of current may be due to high bulk resistance of the polymer, as well as the probable formation of thick oxides of aluminium.

1. *Introduction*

A polymer may be defined as a large molecule consisting of repeating units joined by covalent bonds [1]. Polymer means "many parts", derived from the Greek: polus- (many), meros- (parts). The term macromolecule is a synonym for polymer. The smallest part of a polymer is called a monomer. A monomer is a molecule which combines with other molecules of the same or different type to form a polymer. Oligomer refers to few monomer units. Polymers are arbitrarily arranged and have molecular weights greater than about 5000, but no firm lower limit [2].

A polymer can be organic (made from carbon) or inorganic (made from atoms other than carbon) and also can be natural or synthetic. Cotton, starch, protein, wool etc. are examples of natural polymers, where as nylon, plastics, rubber, fibers etc. are synthetic polymers. Because of their diverse chemical and physical properties, polymers exist from a simple flexible rubber to a hard and brittle glass [3]. Most polymeric materials have been used for decades for the purpose of insulation, specially in electronics industry. Also they are widely applied in automotive industries, in the building construction and in the packing industries. The use of polymers now out stripes that of metals, even cost wise, the polymeric item often comes well ahead of its traditional counter part [4].

Nowadays the concept of polymers as being insulators has changed during the past 20 years. A new class of organic polymers capable of conducting electricity has now emerged. Such materials belong to a class of materials called "synthetic metals". Their conductivity ranges from insulating through semiconducting to metallic. The emergence of such materials arose curiosity of researchers in the field. The discoveries reported reveal that there is a tremendous potential for future scientific and technological applications.

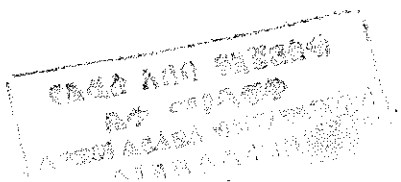

The aim of this research work is to investigate the electrical properties of junction between Aluminium and PDOPT. The sample with which the work has been done has a sandwich structure of the form Al/PDOPT/ITO(Indium doped tin oxide), which is prepared locally. The characterization is done by measuring mainly the current-voltage (I-V) relationship and the complex impedance.

2. *Organic Semiconducting Polymers*

2.1 Conducting Polymers

Conductivity can be described in terms of the density of electrons and their freedom to move. Using these properties, materials may be classified as insulators, semiconductors, conductors or superconductors. The same method holds true for organic materials as well. Until the late 1970, organic polymers were classified as insulators. It came therefore, as a surprise when it was discovered that polyacetylene, $(CH)_n$ [5,6] manifests electrical properties which resemble those of conventional semiconductors or metals. So it has become difficult to categorize $(CH)_n$ as an insulator.

The science of solid state physics, which studies the properties of a well-defined regular array of atoms will be our footing to discuss conducting polymers. A periodic array of lattice atoms is essential for high conductivity. Highly conducting materials are characterized by very low resistivity which is almost linearly dependent on temperature. According to the band theory partially filled band characterizes metals, where as insulators and semiconductors have filled valence band and empty conduction band respectively. It is the wideness of the gap between the valence and conduction bands that enables us to categorize materials as insulators or semiconductors. For semiconductors the gap is narrower and when electrons gain enough thermal energy, or light energy, they will be able to transit to the conduction band. In pure semiconductors, increasing temperature will increase conductivity exponentially [7]. In metals conductivity decreases with increasing temperature. Conducting polymers have a temperature dependence similar to that of semiconductors [8]. This suggests that theories of semiconductors may be applied to conducting polymers.

The conductivity of polymers can be enhanced by introducing charge carriers. This is typically done by reaction with small quantities of electron-accepting or electron-donating

species. Such process is known as, in chemistry language, reduction or oxidation commonly termed "doping" in analogy with the process in conventional inorganic semiconductors. The term p-doping is used for an oxidation reaction of the polymer and n-doping for the reduction reaction of the polymer. Undoped polymers are also semiconductors but doping them creates allowed states in the band gap through which the charge carriers transit.

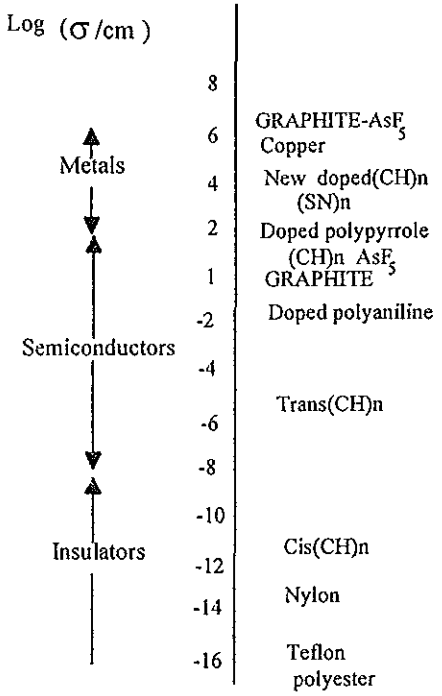

Fig. 2.1.1 Conductivity of polymers as compared with other materials at room temperature.

The process of doping in conducting polymers is not similar to that of conventional semiconductors. In semiconductors doping involves replacing some of the atoms with different species of atoms while in conducting polymers there is no replacement of any atom of the polymer: rather they simply act as associates that accept or donate electrons [9]. Doping

of polymers may be carried out chemically or electrochemically to reach different levels of conductivity.

Organic polymers are applied in the fields like thin film technology, synthetic metals, electroluminescence, non-linear optics and so on. The most extensively studied organic materials, such as polythiophene (PT), polyaniline (PANI), and polypyrrole (PPy) have extended the range of possible applications in the area like polymer light-emiting diodes (PLEDs) [10-12], chemical sensors, field-effect transistor technology, micro-muscles [13], humidity sensors [14], solar cells [15] and so on. There is a hope that in a near future they may be integrated to the existing materials used for these purposes.

Because of some limitations, specially low stability and lack of easy diode processability, the progress in application to fields mentioned above has not been fast enough. After an extensive work, a well defined conjugated polymers (alternating single and double bonds) were able to be synthesized. Their discovery has a great role in pacifying these problems. An alternative successful attempt in overcoming the solubility problem was attaching side chains on the back bone of the conjugated polymer.

Neutral conjugated polymers are insulators or semiconductors. To decrease the band gap of conjugated polymers, different hetrocyclic structures may be introduced. In polythiophene, for example, a variety of side chain subistituents are attached to modify its electronic properties. Figure 2.1.2 depicts some of the substituted polythiophenes having a potential for technological applications.

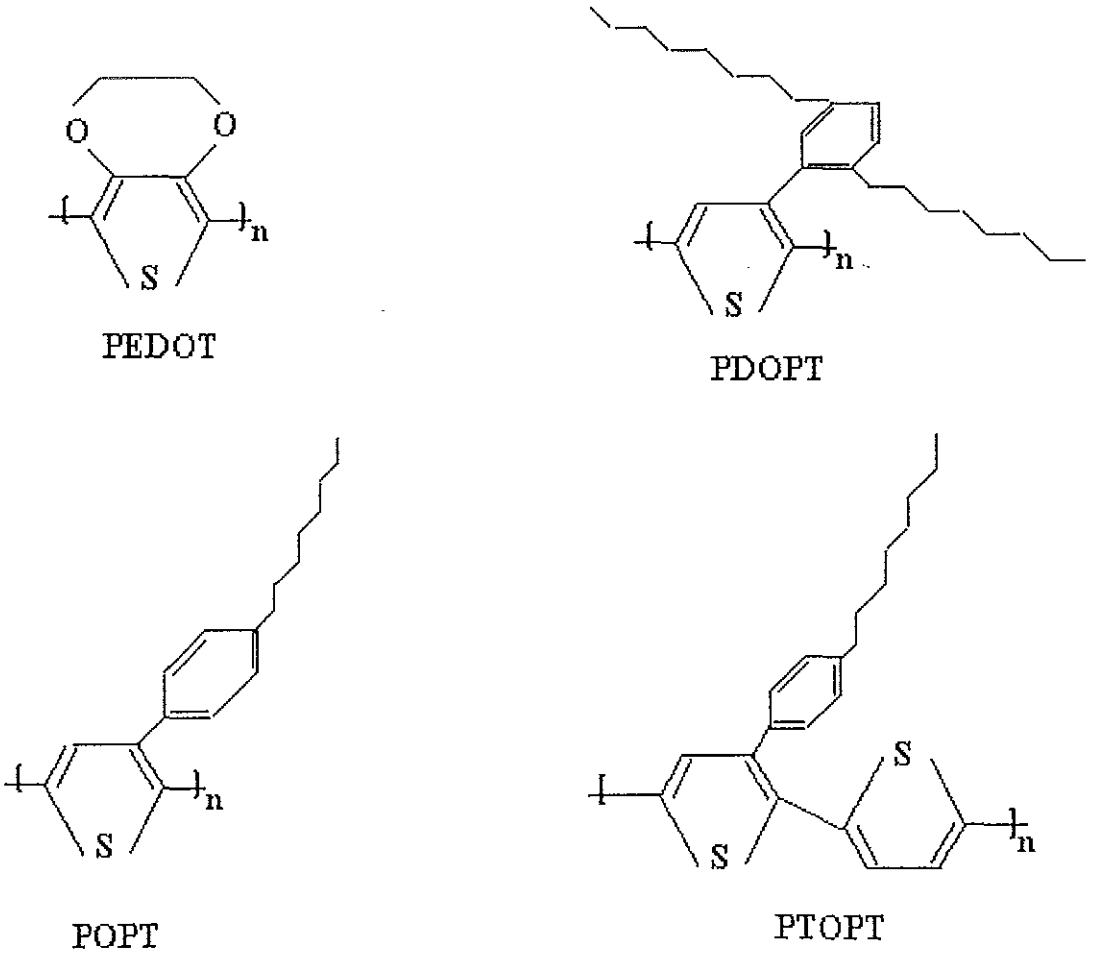

Fig. 2.1.2 Chemical structures of some substituted polythiophenes.

Conjugated polymers are currently considered as materials with a wide range of possible applications, mainly due to their optical and electrical properties. Figure 2.1.3 illustrates chemical structure of some conjugated polymers.

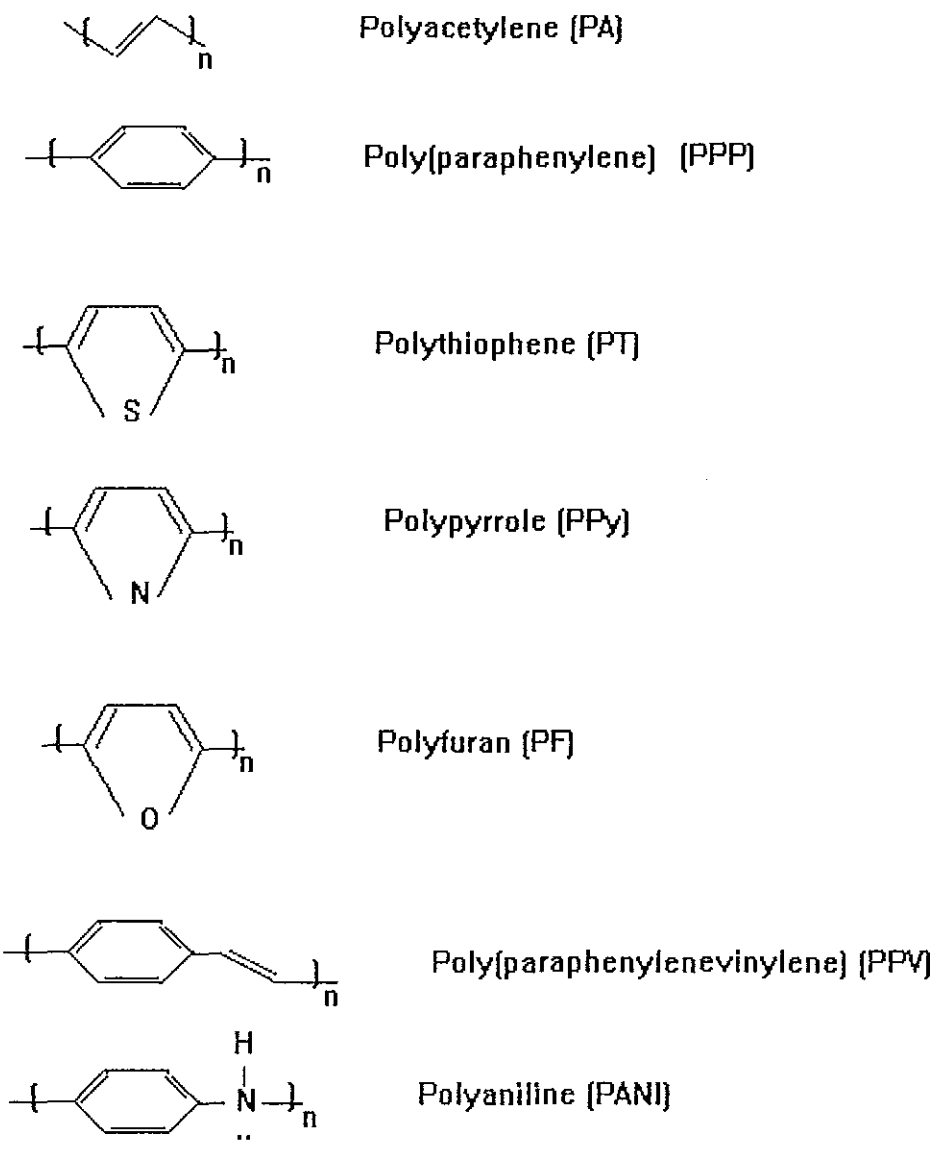

Fig. 2.1.3 Chemical structures of some conjugated polymers.

The chemically simplest type of conjugated polymer is polyacetylene which is polymerized from acetylene monomers. Its conjugation lies only along the main chain between carbon atoms. Its conductivity is the highest of all polymers tested so far, it is linear and hence $(CH)_n$ is taken as a model for a better theoretical understanding of the physical properties of all conjugated polymers. There are two isomers of PA, cis- and trans-. The cis- configuration corresponds to the case when the neighbouring hydrogen atoms are bonded on the same side

of the bond considered, while trans- means neighboring hydrogen bonds are on different sides. Pristine films of PA contain the mixture of these two isomers. The conductivity of trans- form is higher than that of the cis- form. The cis- form of PA has two non-degenerate states where as the trans- form of PA has two degenerate states. The cis- form of PA can be synthesized from gaseous acetylene at -78^{0}C [16] in the presence of appropriate catalyst and can be converted to a trans- form when heated above 150^{0}C [17] as a result of which the conductivity of PA will increase. Figure 2.1.4 shows the isomers of PA with degenerate and non-degenerate states of trans- and cis- forms respectively.

(a)

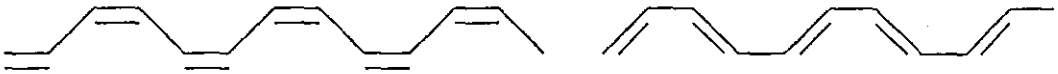

(b)

Fig. 2.1.4 Theoretical isomers of polyacetylene: (a) trans- (b) cis-

2.2 Chemistry and Physics of Conjugated Polymers

Conjugated polymers consist of covalently bonded carbon atoms. Let us briefly see the nature of covalent bonding in terms of atomic and molecular orbitals. A chemical bond is the attraction between atoms in the formation of molecules. Unlike the electrons of isolated atoms, the electrons in molecules are rearranged in such a way that the electrons of one atom is influenced by the nucleus of the other atoms. That is electrons are shared or transfered.

There are two main theories which explain the arrangement of electrons in molecules, the valence band theory (VBT) and molecular orbital theory (MOT). The latter theory is believed to describe precisely the interaction of atoms forming molecules and the distribution of electrons. According to MOT, new molecular orbitals are created when atoms interact during bond formation. The newly created MOs are pairs: bonding and anti-bonding. The bonding MO is of lower energy than either of the parent atomic orbitals. The anti-bonding MO is of higher energy than the original atomic orbitals. Each pair of atomic orbitals gives rise to two molecular orbitals. Combination of s atomic orbitals yields σ (sigma) and σ* bonds.

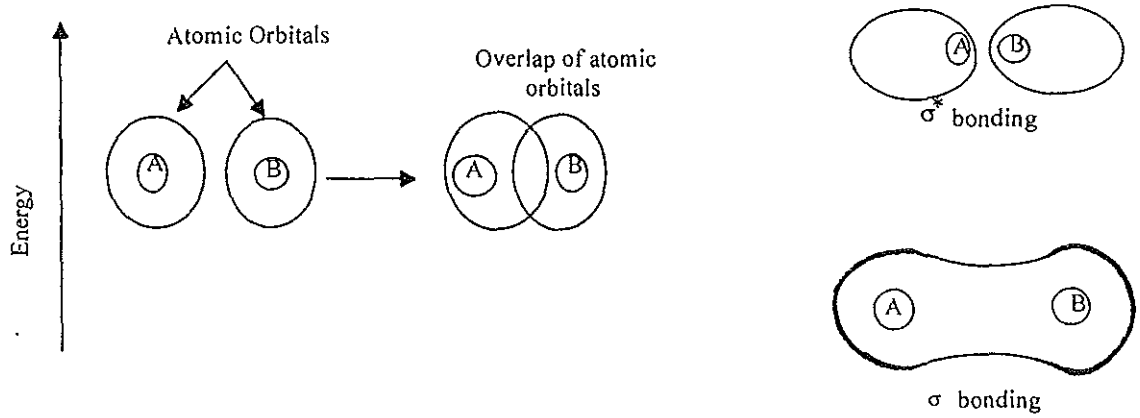

Fig. 2.2.1 Formation of sigma bonds

p atomic orbitals can interact in two ways depending on the spatial distribution of the orbitals. If the atomic orbitals lie along the same axis as in the case p_x-p_x interactions, then a σ MO develops. But if the atomic orbitals have a parallel orientation to each other, i.e. p_y-p_y or p_z-p_z then a π MO will be formed.

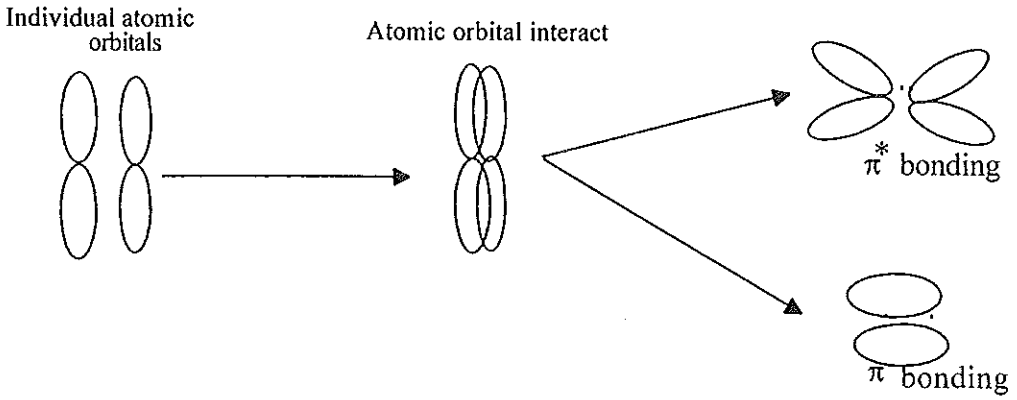

Fig. 2.2.2 Formation of π bond.

Molecular orbitals developed from atomic orbitals of hydrogen atoms are shown in the figure below(fig. 2.2.3). The single electron in each hydrogen atom is accommodated in a 1s atomic orbital. Since the electrons now occupy lower energy levels than they did in an isolated hydrogen atom, the hydrogen molecule is more stable than the isolated hydrogen atoms.

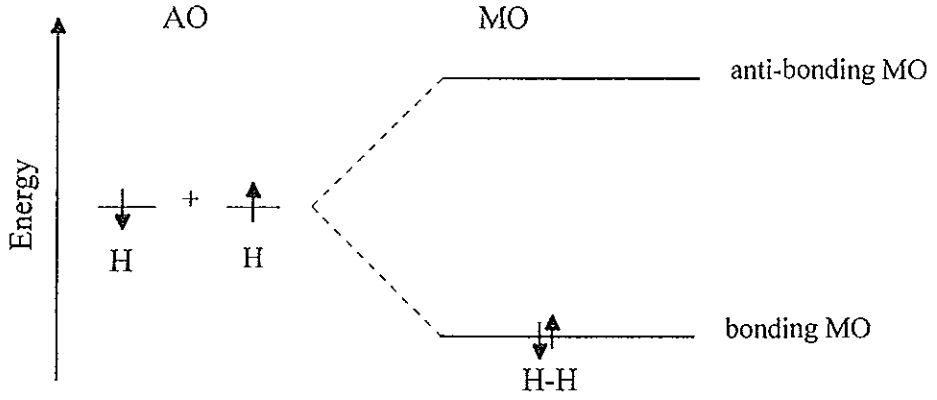

Fig. 2.2.3 Formation of hydrogen molecule.

During bond formation, the atomic orbitals merge together into a new set of orbitals which are known as hybrid orbitals. There are three types of hybrid orbitals.

- ***The sp^3 hybrid orbitals***: In such hybridization the 2s and ($2p_x$, $2p_y$, $2p_z$) electrons are hybridized resulting in four equivalent orbitals arranged tetrahedrally, i.e. pointing towards the four corners of a regular tetrahedron at the center of which is a C atom. Carbon in its ground state has an electronic configuration of $1s^2\ 2s^2\ 2p_x^1\ 2p_y^1\ 2p_z^0$. In its excited state one of the 2s electrons jumps to the empty p orbital, consequently changing the electronic configuration to $1s^2\ 2s^1\ 2p_x^1\ 2p_y^1\ 2p_z^1$. The molecular orbitals of carbon are thus the hybrid formed from one s and three p, i.e. sp^3. If it is combined with four hydrogens of atomic orbitals 1s, four equivalent MOs are obtained for methane. The molecular orbitals are localized since this compound contains only single covalent bonds.

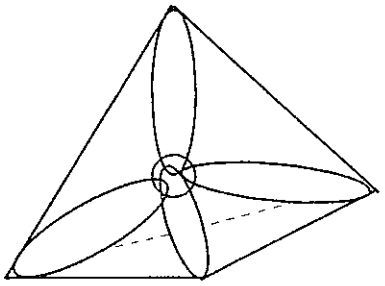

Fig. 2.2.4 Methane formed by sp^3 hybrid orbitals.

- ***The sp^2 hybrid orbitals***: These are resulting from the hybridization of the 2s, $2p_x$ and $2p_y$ orbitals. The remaining $2p_z$ orbital remains unaffected. Thus there will be three equivalent valencies in one plane that form σ-bonds and a fourth pointing at a right angle to this plane which forms a π-bond. The $2p_z$ electrons are known as π-electrons, mobile electrons or unsaturated electrons when they form π-bonds. Such compounds

contain a double bond, which is regarded as being made up of a strong bond (σ-bond) between two sp^2 and a weaker bond (π-bond) between two p_z orbitals.

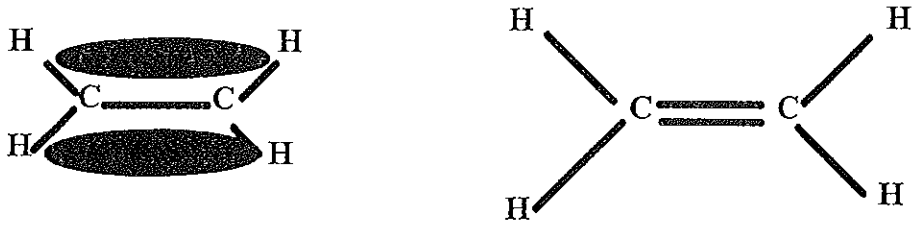

Fig. 2.2.5 Ethylene formed by sp^2 hybrid orbitals.

- ***The sp hybrid orbitals:*** Only one 2s and the $2p_x$ electrons are hybridized resulting in two equivalent collinear orbitals. The $2p_y$ and $2p_z$ electrons remain undisturbed. Thus we get one σ-bond from the sp hybrid and two π-bonds from the p_y and p_z orbitals, eg. acetylene.

Fig. 2.2.6 Acetylene formed by sp hybrid orbital.

Three of the four valence electron orbitals of the carbon atoms in the conjugated main chain namely, one s- and two p- atomic orbitals, are hybridized into three sp^2 orbitals [18]. These three orbitals form σ-bonds to other carbon atoms, hydrogen atoms or others. The remaining

p_z orbital interacts with their neighbors forming π-bonds. So in a conjugated polymer, a single bond (longer) corresponds to a σ-bond where as the double bond (shorter) corresponds to σ + π-bonds.

From solid state physics point of view conjugated polymers are considered as quasi-one-dimensional. Three valence electrons form bonds leaving one free electron per unit cell. The energy band is half-filled, which is analogous to the property of alkali metals. But one-dimensional conjugated polymers with half-filled band are not stable and consequently will undergo transition from metallic to insulator through dimerization [19]. The energy gap separates HOMO (Highest Occupied Molecular Orbital or valence band) from the LOMO (Lowest Unoccupied Molecular Orbital or conduction band). This occurs when the fourth p_z electron is localized there by forming alternating single and double bonds.

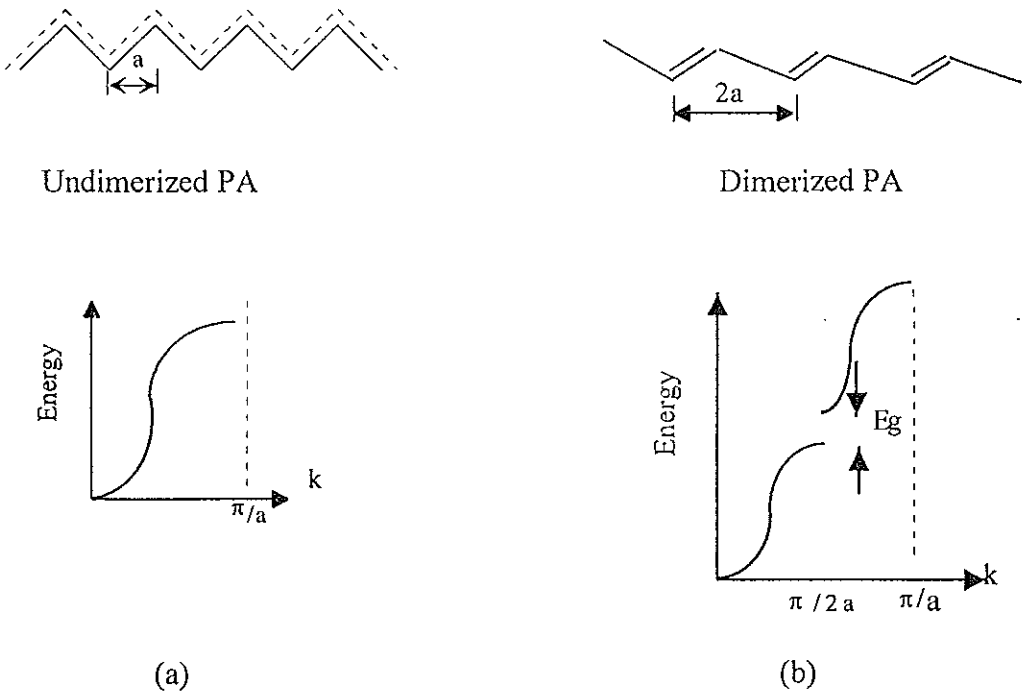

Fig. 2.2.1 Process of transition from (a) metallic state to (b) the dimerized state (non-metallic state) forming a forbidden energy gap.

2.3 *Elementary Excitations*

The existence of stable ground states and excited states of higher energy are the basic assumptions of the modern theory of condensed matters. In most cases the energy of excited states can be expressed as the sum of energies of elementary excitations like phonons (lattice vibration), spin waves (magnons), excitons, polarons, photons, solitons (solitary or "water waves") [20] and so on. Just as atoms, ions or molecules are the building blocks of a crystal in the sense of structure, these elementary excitations are the building blocks of a solid in the sense of motion [20]. In this section we will try to see the concept of elementary excitations in conducting polymers, which are solitons, polarons and bipolarons.

2.3.1 *Solitons in Polyacetylene*

In polyacetylene a soliton is a structural distortion. For the lattice distortion the term 'kink' or 'domain wall' is equivalently used. Figure 2.3.1 shows the two degenerate ground states of trans-polyacetylene.

Phase A Phase B

Fig. 2.3.1 The two degenerate ground states of trans-polyacetylene.

The two phases are energetically equivalent. The kink is a defect where these two phases have a 'misfit' as schematically shown below in Fig. 2.3.2.

Fig. 2.3.2 A broken symmetry in trans-PA creates a soliton.

Due to a strong electron-phonon coupling such defects will introduce a new electronic state in the band gap. This state carries a reversed spin charge relationship: the neutral soliton has a spin, while the charged soliton has zero spin .

Doping will also introduce soliton states. In this process, since there is a transfer of charges, solitons will be charged. As a result the three possible solitons are given below.

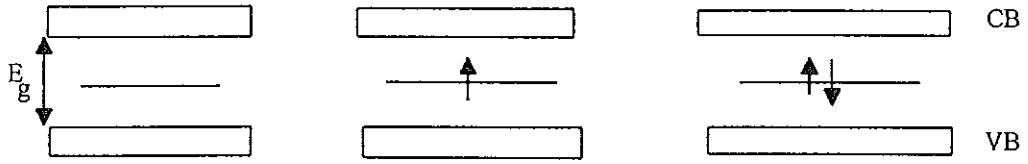

positive soliton	neutral soliton	negative soliton
spin 0	spin 1/2	spin 0
charge +e	charge 0	charge -e

Fig. 2.3.3 Energy band diagrams of polyacetylene with solitons.

Charged solitons do not carry spin, while neutral solitons have spin 1/2.

Photogeneration and charge injection are the two other mechanism of generating solitons.

2.3.2 Polarons and Bipolarons

The motion of electrons in an ionic crystal gives rise to another elementary particle. When an electron is moving in an ionic crystal, its surrounding medium will be polarized with negative ions being repelled away and positive ions being attracted towards it. The polarization field thus produced, in turn, affects the motion of the electron itself. This complex-moving electron and its accompanying polarization field is called a polaron [20]. A polaron is a charge carrier (electron or hole) [21]. Two types of polarons are termed as elementary excitations. These are the small and large polarons. The basic characterizations of these polarons are their electron-phonon coupling and their size. In small polarons, the electron-phonon coupling is very strong, the size of the polaron is comparable to the lattice constant. In large polarons, the electron-phonon coupling is weak and the size of the polaron is large. In conjugated polymers a polaron is used to describe the bound states of the localized electron state and the associated lattice deformation which is soliton and anti-soliton.

As it is stated above, except trans-PA, all other conjugated polymers possess non-degenarate ground states with two possible structures: aromatic and quinoid. The energy of the aromatic structure is lower than that of the quinoid and hence the ground state corresponds to the aromatic type. For polythiophene, form a) in Fig. 2.3.4 is called aromatic and form b) is called quinoid.

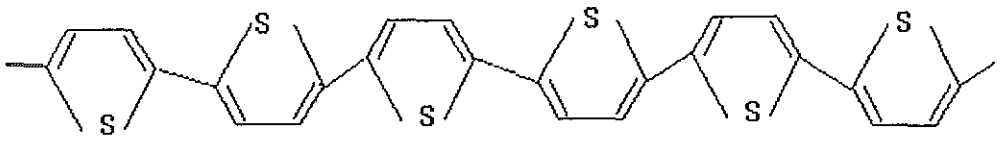

(a)

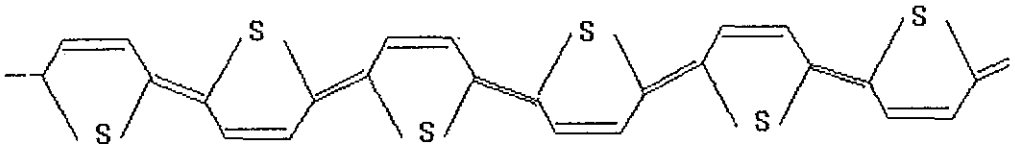

(b)

Fig. 2.3.4 The two forms of polythiophene, (a) aromatic and (b) quinoid.

In a polythiophene, breaking the conjugation at the misfit leads to a transition from aromatic to quinoid state as shown in Fig. 2.3.5 below.

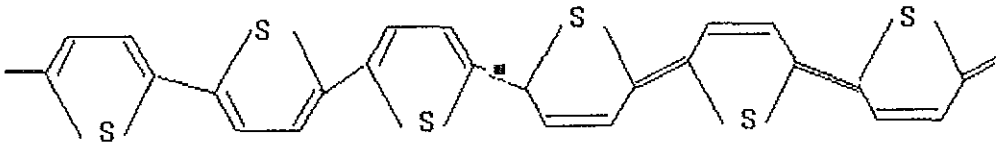

Fig. 2.3.5 Soliton site in a polythiophene.

Unlike solitons in PA which are stable and can be positioned any where in the chain, solitons in non-degenerate polymers are energetically unstable. To stablize the soliton, the bound double defects have to be created and it is this bound double defect which is known as polaron (or removal of an electron from a structure of polythiophene will generate a polaron). Further removal of an electron from the already oxidized polymer containing the polaron results in the generation of a doubly charged state termed as a bipolaron. Polarons and bipolarons are self localized in order to minimize the energy of the main chain and are assumed to extend over four or five rings along the chain [9].

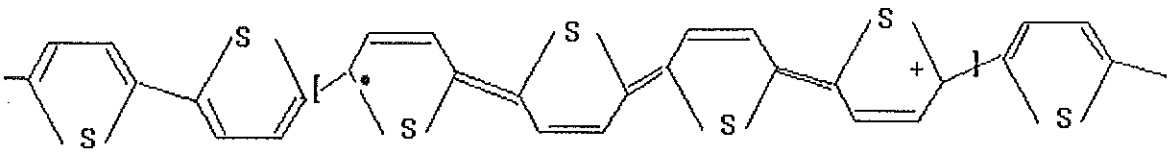

Polaron

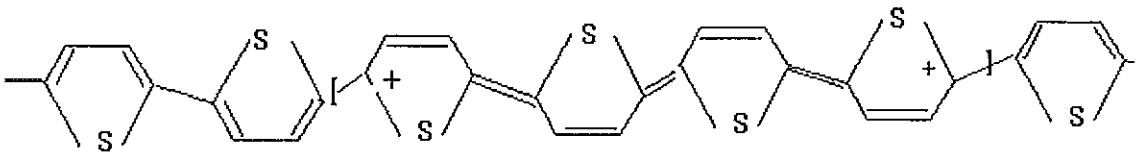

Bipolaron

Fig. 2.3.6 Polaron and Bipolaron in polythiophene.

Bipolarons are usually said to be formed when two polarons meet. Bipolarons are more stable than two polarons: in other words the sum of the energies of two polarons is greater than the energy of a bipolaron. Polarons attract each other; bipolarons repel each other but polarons and bipolarons coexist [21].

Generation of a polaron and a bipolaron creates two interacting states which are energetically separated in the energy gap, unlike the single mid gap state of solitons. Figure 2.3.7 depicts the energy band diagrams of the polaron and bipolaron states. For polarons each level within the gap is singly charged while for bipolarons all the states are empty or full which implies that bipolarons are spinless.

Increasing the doping level will increase the polaron concentration and hence there will be a probability for them to interact and form a more stable bipolaron.

At higher doping levels bipolarons merge with the conduction band (CB) and valence band (VB). In a lightly doped hetrocyclic polymer, it is the spins of the mobile polarons which are the carriers of charge.

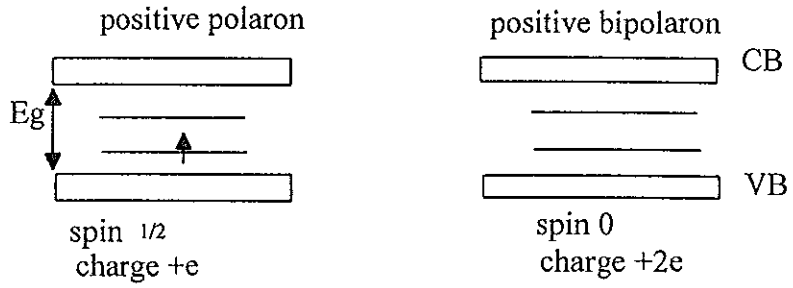

Fig. 2.3.7 Energy band diagrams showing charged states of a non degenerate ground state polymers.

From the above figure we observe that the positive bipolarons make possible new transitions, namely, transitions from the valence band to the two different bipolaron states. In the optical absorption spectrum we find two new peaks, corresponding to the new transitions. The optical transitions due to polarons are seen rarely, since they appear only at very low doping levels and it is energetically favourable to combine polarons and form bipolarons.

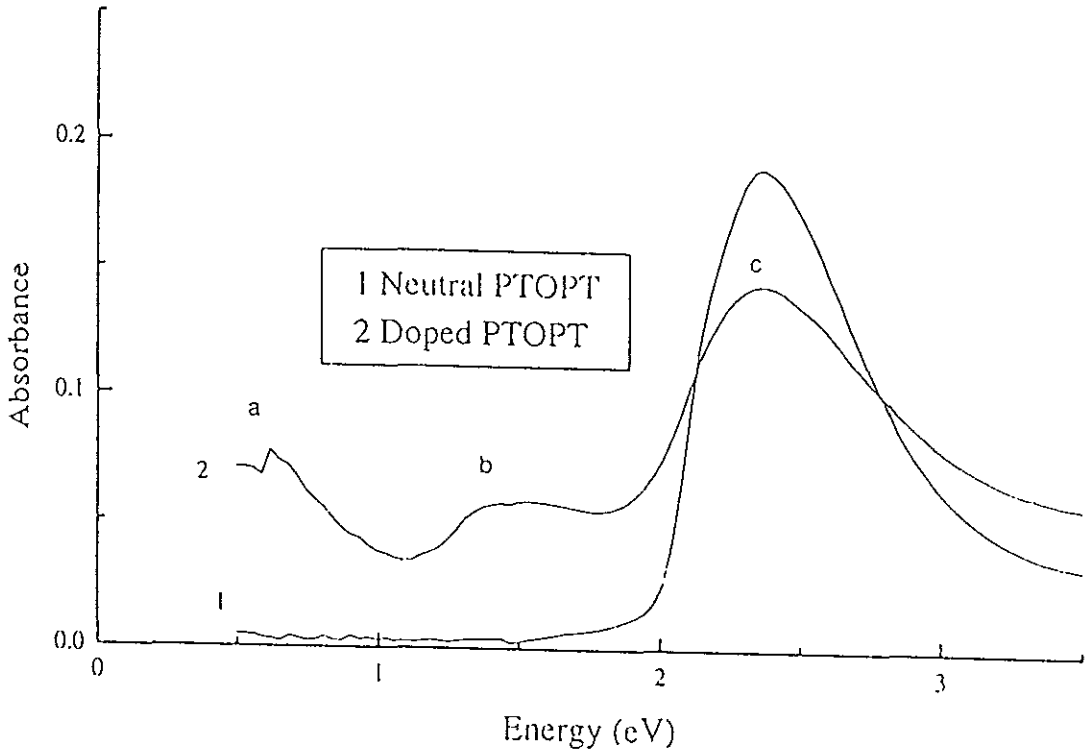

Fig. 2.3.8 Optical absorption spectrum of PTOPT lightly doped with $NOPF_6$.

Labels a, b and c are absorption peaks corresponding to transitions [7].

There is a difference in the conduction mechanism between conducting polymers and inorganic semiconductors. In conducting polymers conduction is possible only via the movement of polarons or bipolarons while the conduction band remains totally empty and the valence band remains totally full. Such a mechanism also requires transport of the negative counterions which must migrate along the polymeric chain to compensate the transport of the positive bipolaronic charges. Therefore, unlike the situation for inorganic semiconductors, the conduction mechanism for polymers involve the movement of both ionic and electronic charges.

2.4 Charge Transport Mechanism and Electrical Conductivity

Neutral conjugated polymers have low conductivity at room temperature. Through doping it is possible to elevate their conductivity by many orders of magnitude for PA [22]. Conductivity depends not only on the doping level [23], but also on temperature [24]. According to Y.W Park et al. [23], the electrical transport mechanism in PA doped with AsF_5 or iodine was explained. Their work covers the full concentration (y), $[CH\ (AsF_5)_y]x$, ranging from undoped to metallic. According to them three regimes exist: the metallic (highly doped) state $y > 0.01$, the transitional region $0.001 < y < 0.01$, and the dilute limit (lightly doped) $y < 0.001$.

The temperature dependence of polymer conductivity is manifested opposite to that of metals. For polymers at low temperature conductivity decreases with decreasing temperature.

There is no definite mechanism of charge transport and hence different models are suggested over the whole conductivity range. In the undoped form of conjugated polymers, the charge transport is similar to that of amorphous semiconductors. It is explained by hopping between localized states according to hopping or variable range hopping theory. Variable-range-hopping (VRH) is a thermally activated hopping between localized states near the Fermi level. At very low doping levels, the conductivity is mainly due to hopping (phonon assisted quantum mechanical tunneling). Its concept is generally deduced from ionic conduction to electronic conduction in amorphous and disordered non-metallic solids and polymers. In such materials we do not have free charge carriers, rather localized electrons and so they can move between these localized states which are distributed randomly.

The hopping probability in the presence of an electric field is given by

$$\nu_{hop} = \nu_{ph} \exp\left[-2\alpha R - (W \pm e\varepsilon R)/k_B T\right] \qquad (2.4.1)$$

where α^{-1} is the decay length of the localized state wave function.

R is the distance between the two sites (hopping distance).

W is the energy difference between the states (potential barrier).

ε is the electric field.

k_B is the Boltzmann constant.

T is the absolute temperature.

ν_{ph} is the hopping attempt frequency.

The plus or minus sign corresponds to hopping along or opposite to an electric field, respectively.

If the external field is weak, i.e. $e\varepsilon R << k_B T$, the hopping conductivity is given by [20].

$$\sigma = 4e^2R^2 \nu_{ph} N(E_F) \exp[-2\alpha R - W/k_B T] \qquad (2.4.2)$$

where $N(E_F)$ is the density of states.

Here we have two conditions corresponding to two types of hopping. If the localization is very strong, i.e. $\alpha R_o >> 1$, where R_o is the nearest neighbour distance, only nearest neighbour hopping is possible. If αR_o is less than or equal to one (or at very low temperature) then the variable range hopping is expected to dominate.

The temperature dependence of conductivity in 3-dimensions is given by:

$$\sigma(T) = \sigma_o \exp\left[(-T_o/T)^{1/4}\right] \qquad (2.4.3)$$

where T is the absolute temperature and T_o is constant.

This model has been shown to be appropriate for polyacetylene, poly(3-alkylthiophene) [25], and polypyrrole [26]. Other models are shown to be useful as we go to higher doping levels

and conductivities. Such a model is proposed by Sheng and co-worker [27-28] and according to them the distribution of localized states tends to form clusters, then the conductivity can be described by thermally activated voltage fluctuation across the junction which influences the tunneling probability. Thus the model gives the temperature dependence of the conductivity as:

$$\sigma(T) = \sigma_o \exp\left[-T_o/(T+T_1)\right] \qquad (2.4.4)$$

where the constants T_o and T_1 are determined by the shape and size of the insulating barriers. This model assumes large conducting islands separated by a potential barrier, which is to mean the co-existence of doped and undoped regions in a conjugated polymer.

Very recently, a Drude type metallic behaviour of conducting PPy [29] and polyaniline [30] is reported, where an insulator to metal transition occurs.

3. *Electrical Properties of Metal/Semiconductor(MS) and Metal/Insulator/semiconductor(MIS) Contacts*

3.1 Current-Voltage Characteristics

Devices made of contacts between metal and semiconductors play a major role in the modern technological applications. The fabrication of devices such as rectifiers, point contact diodes, metal semiconductor field-effect transistors etc. are based on the metal semiconductor contacts [31]. The contacts between the metal and the semiconductor can be ohmic or non-ohmic depending on their work functions. The non-ohmic contact may be a rectifying contact (Schottky barrier).

The current-voltage properties of many rectifying metal-semiconductor contacts can be described by the thermionic emission/diffusion equation given below [32].

$$J = J_o \left[\exp(qV/nk_BT) - 1\right] \qquad (3.1.1)$$

where J is the total current density, J_o is the value of the reverse saturation current density, q is the charge of the electron, V is the applied voltage, n is the diode ideality factor, k_B is Boltzmann's constant and T is the absolute temperature. In a rectifying contact there is a one way well favoured flow of current, that is, when the metal semiconductor contact is forward biased for which $J >> J_o$. When it is reverse biased, there will be a very small value of the current. The flow of charge carriers will be blocked by the large barrier height. Better rectification is observed for decreasing values of the reverse saturation current density J_o as compared to J.

At the other extreme, when J_0 is very large compared with J, the junction will readily pass current for both signs of the applied voltage. The above equation of a diode (eqn. 3.1.1), for $J_0 >> J$, can be expanded to yield:

$$V = \left(nk_BT/qJ_o\right) J \qquad (3.1.2)$$

This equation is a linear, ohmic response displayed by the metal/semiconductor contact system.

Between the two conditions, the current-voltage characteristics appear as a mixture of this limiting cases, i.e., symmetrical, non-ohmic and non-rectifying. Ohmic contacts are equally important in many applications of semiconductor devices because of small ohmic losses. The communication between semiconductor devices or integrated circuits, and the outside world is via ohmic contacts which is a low resistance junction [33]. The rectifying contacts are desirable for photovoltaic cells, photodetectors, field-effect transistors [31], and other semiconductor devices.

The physics remains unaltered in using conjugated polymers instead of inorganic semiconductors in the metal semiconductor contact. When a semiconductor of a given work function is brought in contact with a metal having a different work function, charge will flow across the interface to create equilibrium. It is the direction of the flow of this charge that determines the electrical properties of the device. Immediately after the contact between the metal and the semiconductor, their Fermi levels will attain equilibration, i.e., the same value. Based on the relative magnitudes of the work functions, the energy edge of the semiconductor bends near the interface as shown in Fig. 3.1.1. A p-type semiconductor-metal junction, where if the Φ_m (metal's work function) is less than Φ_s (semiconductor's work function), a rectifying junction is formed while if $\Phi_m > \Phi_s$ an ohmic junction is formed [34]. The same phenomena are observed [35] for a p-type semiconducting polymer-metal interface.

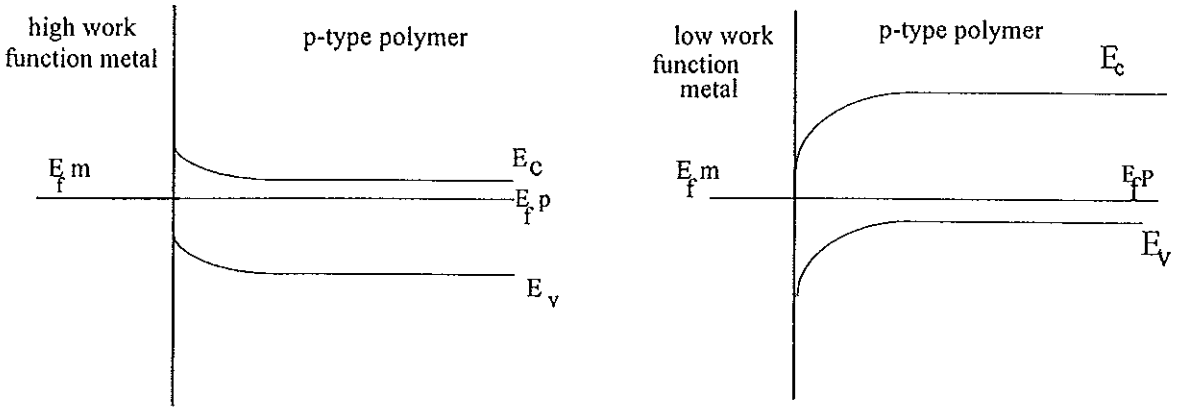

Fig. 3.1.1 Band structure of junctions between a p-type polymer and a metal with high work function (left), and low work function (right).

In Fig. 3.1.2, we observe the formation of a depletion layer of width W between a metal and an n-type semiconductor. The values of band edge energies E_c and E_v are distance-dependent in the depletion region, whereas the Fermi level remains unaffected in both regions ($E_{fm} = E_{fs}$).

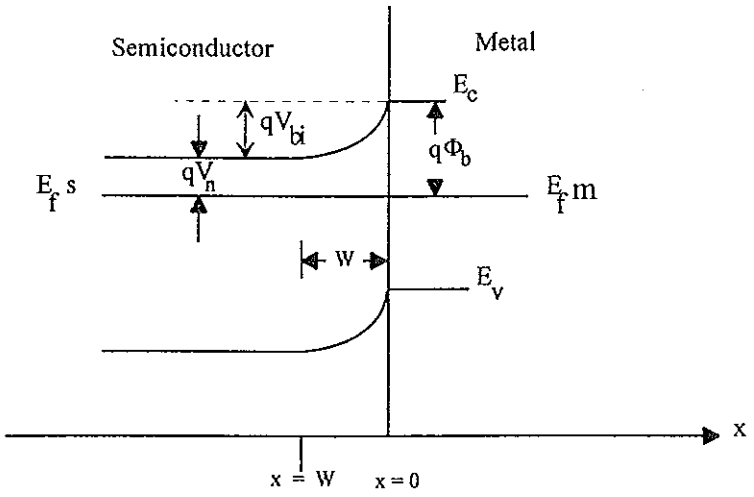

Fig. 3.1.2 Energy band diagram with important parameters.

To determine the value of J_o, the reverse saturation current density, we have to define the following parameters.

qV_n is the distance between E_f and E_c in the bulk of the semiconductor.

V_{bi} is the in-built potential of the junction.

Φ_b is the barrier height. $\Phi_b = V_n + V_{bi}$.

For inorganic semiconductor/metal contacts, an explicit relationship between the barrier height and J_o can be obtained from thermionic emission theory [31].

$$J_o = A^{**} T^2 [\exp(-q\Phi_b / kT)] \qquad (3.1.3)$$

where A^{**}, which is known as the modified Richardson constant, expresses [7]:

i) the number of electrons at the semiconductor-metal interface that is injected into the metal and ii) the effective density of states in the conduction band, the effective mass of electrons in the semiconductor, phonon scattering and quantum mechanical reflection at the semiconductor-metal interface. q is the electric charge, and T is the absolute temperature. The value of A^{**} is typically between 10 and 100 $Acm^{-2} K^{-2}$. But for free electrons the Richardson constant A = 120 $Acm^{-2}K^{-2}$. De Leeuw et al. [36] have taken the value of Richardson constant as that of free electrons for organic semiconductor Schottky diodes. So the value of J_o can be obtained by extrapolating the linear part of the plot of lnJ vs. V and taking the intercept with the J-axis. Thus one can determine the barrier height (Φ_b), knowing the value of T.

The contacts between electropositive (low work function) metals and n-type semiconductors, or contacts between electronegative (high work function) metals and p-type semiconductors, will result in the formation of a low barrier height for which J_o is large and hence the contact is ohmic. High barrier height and low J_o is obtained for contacts between low work function metals and p-type semiconductors or for contacts between high work function metals and n-type semiconductors.

3.2 Capacitance-Voltage Measurement

The barrier height can also be determined by the capacitance measurement. The capacitance of the depletion layer (Fig. 3.1.2) of a reverse biased semiconductor is given by :

$$C = A_S \left[(q\varepsilon_S N_d / 2)^{1/2} (\Phi_b - V_n - V - kT/q)^{-1/2} \right] \qquad (3.2.1)$$

where A_S is the cross-sectional area of the device,

ε_s is the dielectric constant of the semiconductor,

N_d is the dopant density of the semiconductor,

V is the applied voltage and

kT/q is the thermal energy (in volts).

If we rearrange the above equation we get:

$$1/C^2 = \{2/ (qA_S^2 \varepsilon_S N_d)[\Phi_b - V_n - V - kT/q]\} \qquad (3.2.2)$$

From a plot of $1/C^2$ against V, the barrier height can be determined from the intercept with the voltage axis, i.e.

$\Phi_b - V_n - kT/q = V_i$, where V_i is the voltage intercept. Hence:

$$\Phi_b = V_i + V_n + kT/q \qquad (3.2.3)$$

The slope of the graph enables us to determine the carrier density (dopant concentration) if the dielectric constant of the semiconductor is known.

Metal-insulator-semiconductor diodes have great importance in device physics. Such a structure is reported [37] for conjugated polymer-metal junctions. The insulating surface is reported to be formed while depositing on a low work function metal (Al).

3.3 Impedance Spectroscopy

Impedance Spectroscopy (IS) is a new and powerful [38] method of characterizing the electrical properties of materials and their interfaces with conducting electrodes. It may be used to investigate the dynamics of bounded or mobile charges in the bulk or interfacial region of any kind of solid or liquid materials that conducts ionically, or semiconductors, mixed electronic-ionic conductors and even insulators (dielectrics). There are various types of electrical responses which are used in IS, out of which we focus only on the technique which is standard and most common that enables us to measure impedance directly as a function of frequency by applying a known voltage, or current to the sample and measure the phase difference and amplitude, or real and imaginary parts of the resulting current or voltage.

Suppose the signal applied to the sample is $V(t) = V_m \sin(\omega t)$, involving a single frequency, $f = \omega/2\pi$ and the resulting current $I(t) = I_m \sin(\omega t + \theta)$ will be measured, where θ is the phase difference between the voltage and the current. The phase shift is $\theta = 0$ for pure resistors and $\theta = \pi/2$ for pure capacitors. The electrical circuit with a combination of resistors and capacitors, therefore manifests the phase difference between 0 and $\pi/2$. Impedance is defined as

$$Z(\omega) = V(t) / I(t) \qquad (3.3.1)$$

Its magnitude is $|Z(\omega)| = V_m / I_m$ and its phase angle is $\theta(\omega)$, a function of ω.

Impedance is a more general concept than resistance, since it takes into account the phase difference. It can be represented by a rotating vector diagram in a complex rectangular or polar coordinate system. The magnitude and direction of impedance can be obtained from its planar vector representation

$$Z = Z' + jZ'' \qquad (3.3.2)$$

Where $j = \sqrt{-1} = \exp(j\pi / 2)$.

$$Re(Z) \equiv Z' = |Z| \cos(\theta) \qquad (3.3.3)$$

and

$$Im(Z) \equiv Z'' = |Z| \sin(\theta) \qquad (3.3.4)$$

with the phase angle

$$\theta = \tan^{-1}(Z''/Z') \qquad (3.3.5)$$

and the modulus $$|Z| = [(Z'')^2 + (Z')^2]^{1/2} \qquad (3.3.6)$$

In polar form $Z(\omega) = |Z| \exp(j\theta)$. Impedance is by definition a complex quantity and is only real when $\theta = 0$. Quantities such as admittance Y, modulus M, and dielectric permitivity ε, which are related to the impedance Z often play an important role in IS. Usually all of them are generally called immitance.

Admittance $Y \equiv 1 / Z \qquad (3.3.7)$

and

$$Y \equiv Y' + jY'' \qquad (3.3.8)$$

In terms of capacitive and resistive components:

$$Z = R_s(\omega) - jX_s(\omega) \qquad (3.3.9)$$

and

$$Y = G_p(\omega) + jB_p(\omega) \qquad (3.3.10)$$

where the reactance $X_s \equiv [\omega C_s(\omega)]^{-1} \qquad (3.3.11)$

and the susceptance $B_p \equiv \omega C_p(\omega) \qquad (3.3.12)$

and the conductance $G_p = R_p^{-1} \qquad (3.3.13)$

The subscripts s and p stand for series and parallel, respectively. If we expand the equation of admittance, we get

$$G + jB = 1/(R+jX)$$

$$= (R - jX) / (R^2 + X^2) \qquad (3.3.14)$$

$$G + j\omega C_p = \{R + j/\omega C_s\} / \{R^2 + 1/\omega^2 C_s^2\} \qquad (3.3.15)$$

where C_s (= $-1/\omega X$) is the equivalent series circuit capacitance. $C_p = B/\omega$ is the equivalent parallel circuit capacitance. Obviously, if no series resistance (R) and parallel conductance (G) are present, the equivalent series circuit capacitance (C_s) and equivalent parallel circuit capacitance (C_p) are identical [39].

The following table summarizes the relation between the four basic immittance functions for a sample containing only a capacitor with capacitance C.

	M	Z	Y	ε
M	M	μZ	μ/Y	1/ε
Z	μ^{-1}M	Z	1/Y	1/με
Y	μ^{-1}M	Z^{-1}	Y	με
ε	1/M	$\mu^{-1}Z^{-1}$	μ^{-1}Y	ε

where $\mu = j\omega C$

Table 3.3 Relation between immittance functions.

It is not only Z that can be drawn on the Agrand diagram, but also Y, M & ε. The main purpose of this sub-section is that, observing the impedance response of our sample, we will be able to model its equivalent electric circuit. For example, if we consider a circuit with RC in parallel, the impedance of the circuit may be expressed as in the following. For a capacitive reactance one can use the following relation.

$$CV = Q \qquad (3.3.16)$$

Where Q is the stored charge in coulomb.

Hence

$$I = \frac{dQ}{dt} \qquad (3.3.17)$$

But $V = V_0 \exp(j\omega t) = V_0(\cos\omega t + j\sin\omega t)$. So substituting this in (3.3.16)

$$I = CV_0 \frac{d}{dt}(\cos\omega t + j\sin\omega t)$$

$$= \omega V_0 C(-\sin\omega t + j\cos\omega t) \qquad (3.3.18)$$

Therefore the capacitive reactance will be the ratio of V to I. That is

$$X_c = V_0(\cos\omega t + j\sin\omega t) / \omega V_0 C(-\sin\omega t + j\cos\omega t)$$

If we multiply the denominator with its complex conjugate, we obtain

$$X_c = 1/j\omega C \qquad (3.3.19)$$

Hence the impedance for RC in parallel will be

$$Z = R/(1 + j\omega RC) \qquad (3.3.20)$$

but $RC = \tau$, which is the relaxation time.

Therefore,

$$Z = R/(1 + j\omega\tau) \qquad (3.3.21)$$

$$Re\{Z\} = R/(1 + \omega^2\tau^2) \qquad (3.3.22)$$

$$-Im\{Z\} = R\omega\tau/(1 + \omega^2\tau^2) \qquad (3.3.23)$$

But $\omega\tau = \tan\theta$ and hence

$$Re\{Z\} = R\cos^2\theta \qquad (3.3.24)$$

and

$$-Im\{Z\} = R\sin\theta\cos\theta \qquad (3.3.25)$$

Using a trigonometry identity

$$Re\{Z\} = R[1 + \cos 2\theta]/2 \qquad (3.3.26)$$

$$-Im\{Z\} = R[\sin 2\theta]/2 \qquad (3.3.27)$$

$(R \sin 2\theta)/2$ is maximum for $2\theta = \pi/2 = 90^0$, for which $-Im\{Z\}$ is maximum, i.e. R/2 and $\omega\tau = \tan 45^0 = 1$. The Cole-Cole plot of this circuit will be a semicircle whose center lies on the $Re\{Z\}$ axis [40].

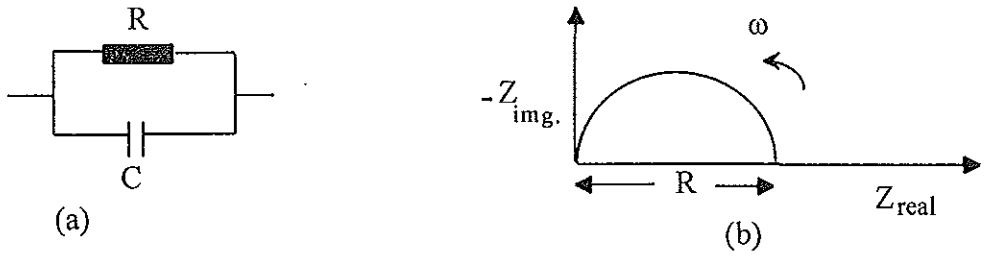

Fig. 3.3.1 Representation of (a) RC in parallel circuit and (b) Z of RC in parallel in a complex impedance plane.

If R and C are in series, its representation in complex impedance plane is shown below.

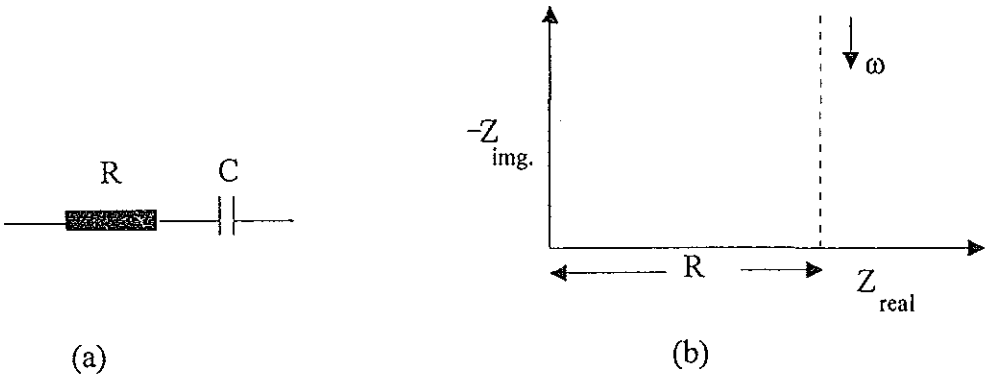

Fig. 3.3.2 Representation of (a) R and C in series circuit and (b) their Z in a complex impedance plane.

If a pure resistior R or a pure capacitor C is used in the circuit, their representation in complex impedance plane will be as shown below.

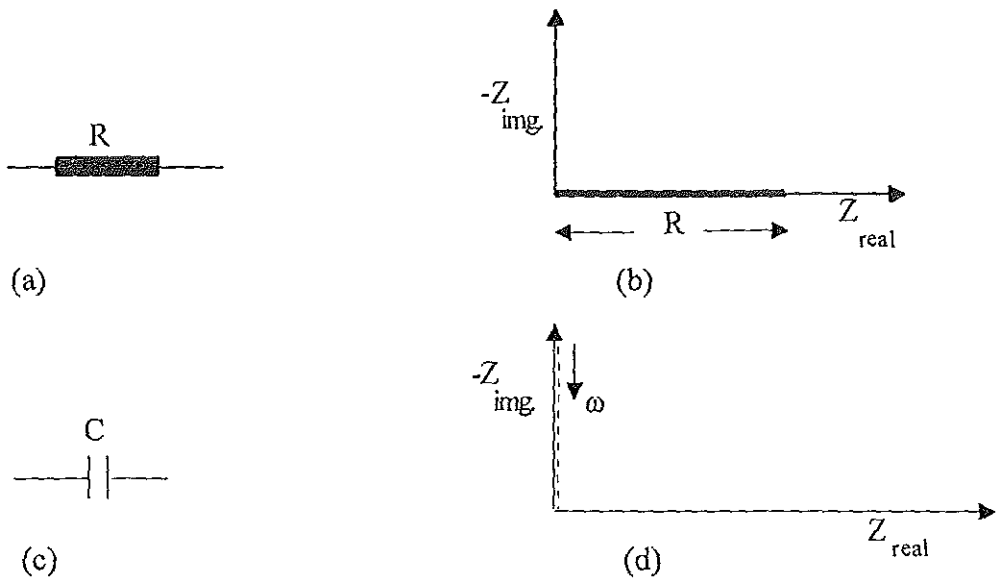

Fig. 3.3.3 Representation of (a) pure resistor in a circuit and (b) its Z representation in complex impedance plane, (c) pure capacitor in a circuit and (d) its Z representation in complex impedance plane.

The parallel RC circuit is an equivalent circuit model for a junction between a metal and a semiconductor representing either the depletion region and/or the thin insulating region at the interface. Two slightly overlapping semicircles are observed for MIS structures [37]. This can be modelled as shown below.

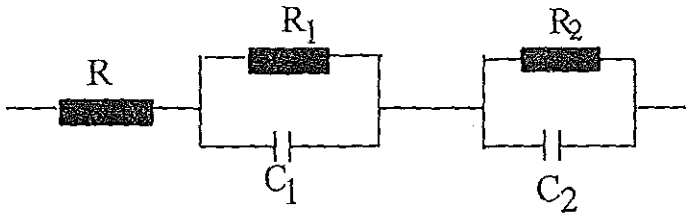

Fig. 3.3.4 An equivalent RC circuit of MIS devices.

The complex impedance of the above circuit is given by:

$$Z = R + R_1/(1 + j\omega R_1 C_1) + R_2/(1 + j\omega R_2 C_2) \qquad (3.3.28)$$

where R is the series contact resistance,

R_1 and C_1 are the resistance and capacitance of an interfacial insulating thin layer and R_2 and C_2 are for the depletion region.

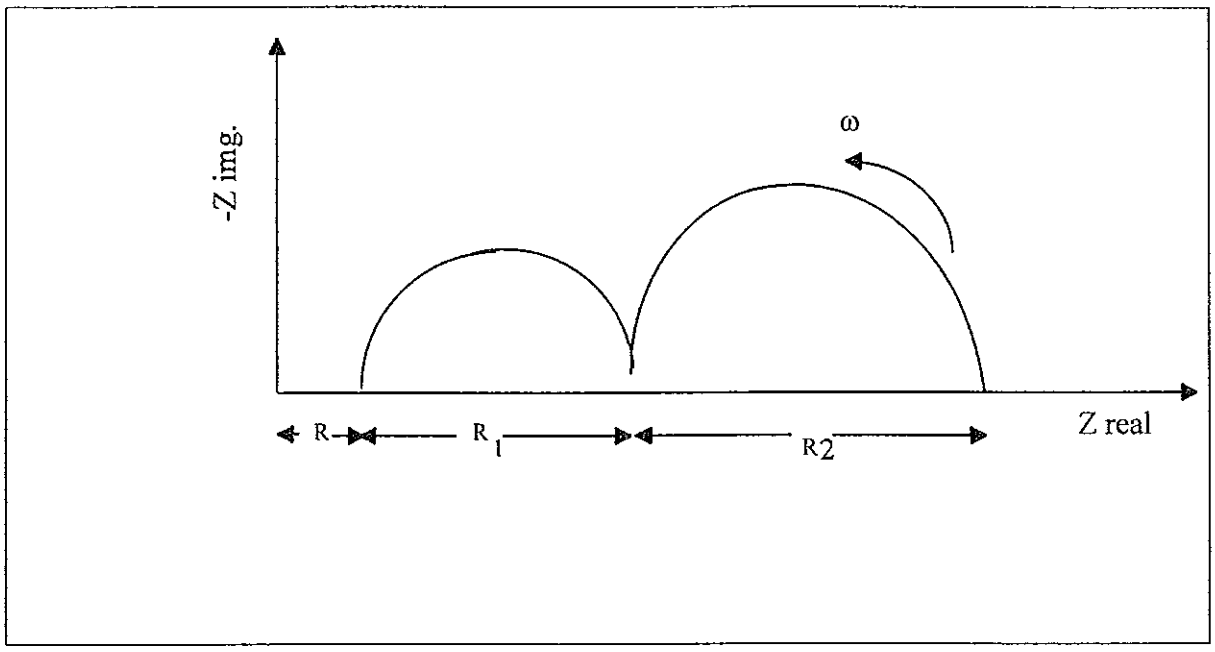

Fig. 3.3.5 Idealized Cole-Cole plot for a circuit modelled as MIS.

4. *Instrumentation and Experiment*

4.1 Instruments

Here we will briefly discuss the systems and functions of the instruments used both for the sample preparation and sample characterization.

4.1.1 The Spinner System

This instrument is used to spin coat the polymer on the ITO/glass substrate. The thickness of the deposited polymer is controlled by the rate of revolution it makes per minute. For a given polymer solution concentration, the higher the speed (rpm), the thinner the deposited polymer.

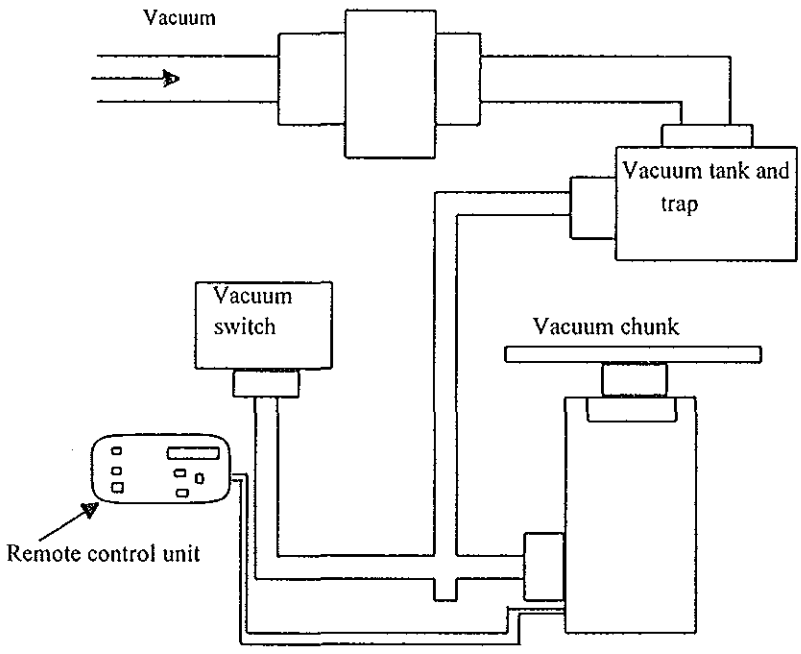

Fig. 4.1.1 Block diagram for the spinner system from reference [41].

4.1.2 Edwards Auto 306 Vacuum Depositor

The Auto 306 is a microprocessor controlled vacuum coater that can be arranged in a variety of coating tasks. The main elements of AUTO 306 are:

- A vacuum pumping system (Diffusion pump),
- A microprocessor control system and control panel,
- A base plate,
- An electrical system,
- Cabinet.

This instrument is designed for thermal vapour deposition processes under high vacuum of the order of 10^{-7} Torr. The thickness of the deposited film is controlled by the sputtering time. The main components of Edwards Auto 306 are given in figure below.

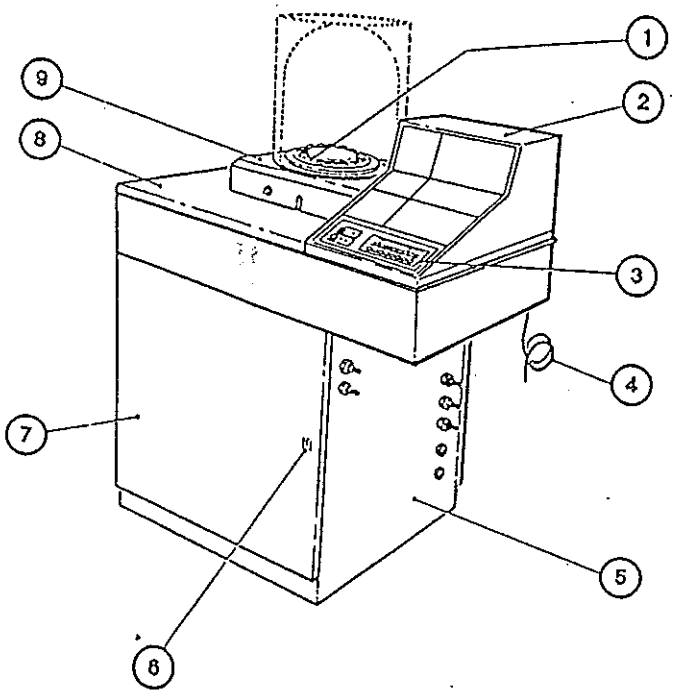

1. Baseplate
2. Electrical Control Cabinet
3. Controller
4. Mains Lead
5. Service Panel
6. Lock
7. Front Door Panel
8. Work Top
9. Baseplate Shroud

Fig. 4.1.2 Main components of Edwards Auto 306 from reference [42].

4.1.3 Perkin Elmer λ19 Spectrophotometer

The Perkin Elmer λ19 UV/VIS/NIR spectrophotometer (Fig. 4.1.3) is a fast and powerful machine for measuring the reflectance, transmittance and absorbance of layers as a function of wavelength or energy. The PE λ19 Spectrophotometer allows spectral measurements between 170 nm and 3200 nm [43].

Description of Fig. 4.1.3

-HL is Halogen lamp that produces VIS/NIR light

-DL is Deuterium lamp that produces UV light

-Mi stands for mirror number "i"

-FW stands for Filter wheel that filters light from the source

-SA is a slit

-Monochr. is an abbreviation for monochromator

-C is a chopper that divides the single beam in to two

-BM stands for Beam Mask

-In the sample chamber there are two ports where R, the reference sample holder and S, the sample holder are installed

-In the detector compartment, two types of detectors exist. PMT (photo multiplier tube) that detects UV/VIS light and PbS (Lead sulfide semiconductor) detector that detects NIR light.

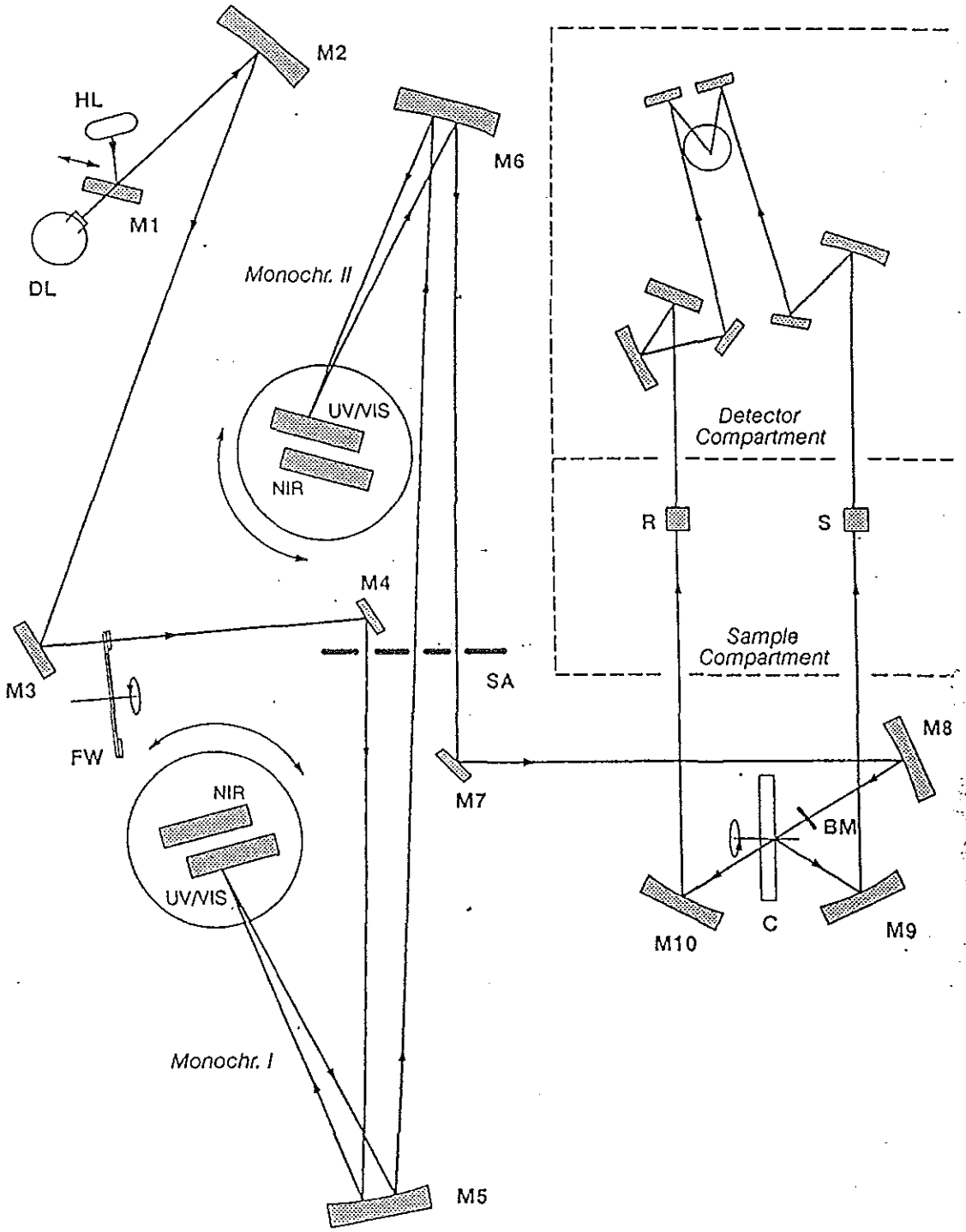

Fig. 4.1.3 Schematic diagram of PE λ19 spectrophotometer.

It is very decisive to use this instrument to study the spectral response of absorption of neutral or doped polymers. In Fig. 4.1.4 absorption spectra of PTOPT is depicted as measured by PE λ9 spectrophotometer [44]. The spectra are rich in information like doping levels, band gap of PTOPT, energy levels of band gap states, etc.

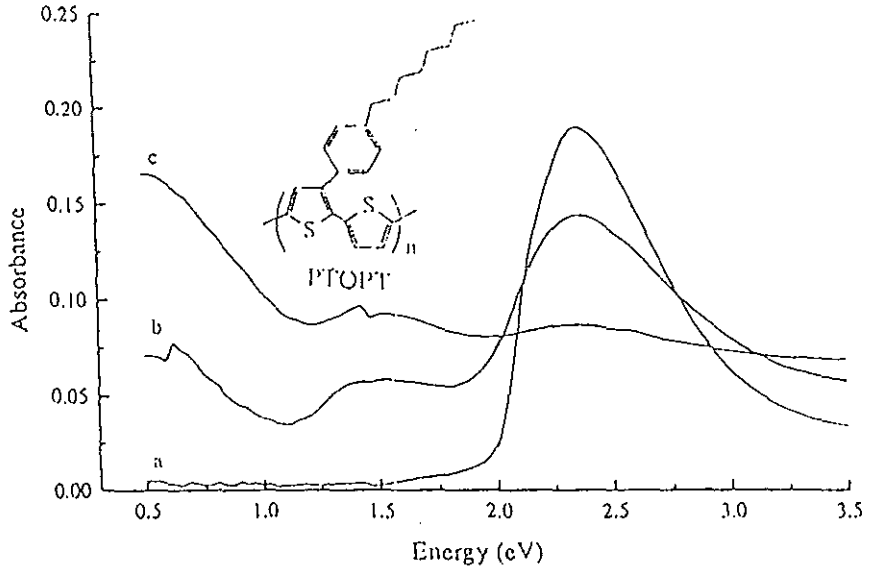

Fig. 4.1.4 Optical absorption spectra of (a) neutral, (b) lightly doped, and (c) heavily doped PTOPT [44].

4.1.4 HP LF 4192A Impedance Analyzer

The HP 4192A Low Frequency impedance Analyzer is a fully automatic, high performance test instrument designed to measure a wide range of impedance parameters. The selected measurement parameters are directly displayed in the display units A and B. Under normal condition this machine performs about five measurements per second.

This machine provides:

- the measuring frequency ranging from 5 Hz to 13 MHz with 1 mHz resolution.

- the oscillation level that varies from V_{rms} = 5 mV to 1.1 V with a resolution of 1 mV for the oscillation level of below 100 mV, and 5 mV for an oscillation level above 100 mV.
- the internal dc bias voltage source varying between -35 V and +35 V.
- The measuring frequency or biasing voltage can be swept automatically or manually, in forward or backward direction.

In immitance measurements, this machine can measure the following impedance parameters.

- Absolute value of impedance ($|Z|$)
- Absolute value of admittance ($|Y|$)
- Phase angle (θ)
- Resistance (R)
- Reactance (X)
- Conductance (G)
- Susceptance (B)
- Inductance (L)
- Capacitance(C), etc.

The zero offset adjustment function measures the residual impedance and stray admittance inherent to the test fixture used, and offsets the effect of these parasitic parameters to zero with respect to the measured value [39].

Recently different publications are appearing on the sandwich structure of METAL/POLYMER/METAL as to understanding the nature of junction and obtaining their equivalent circuit models. Figure 4.1.5 shows the Cole-Cole plot obtained from impedance analyzer for polypyrrole doped with large polymeric anions.

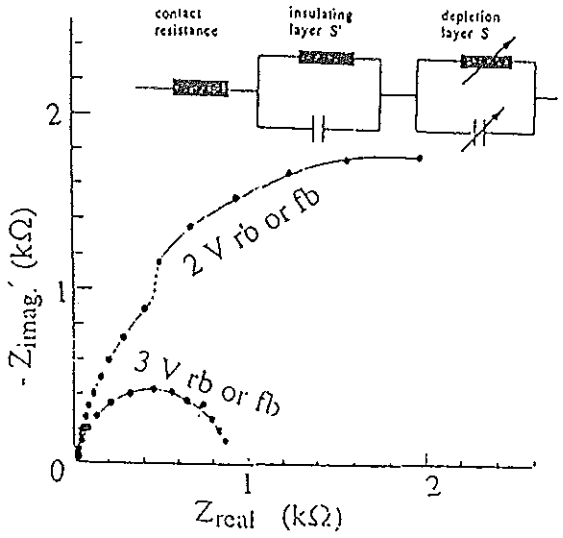

Fig. 4.1.5 Cole-Cole Plots from reference [45].

4.1.5 The pico-Ampere Meter/ DC Voltage Source

Model 4140B pA meter/DC voltage source has high stability with 10^{-15}A (max.). This meter has a basic accuracy of 0.5% over wide measurement ranges. Its application is not limited in the measurement of small leakage currents of semiconducting devices but also for making insulation resistance/leakage and current absorption measurement/analysis of capacitance [46]. The DC Voltage source has an output range between -100 V and +100 V. It is generated either in the stair case or ramp mode. The sweep can be done automatically or manually. For I-V measurements timing is synchronized automatically between the dc voltage source and the pA meter section. The start, stop or step voltages can be set from -100V to +100V at 100 mV resolution or from -10V to +10V at 10 mV resolution. This device can also measure C-V characteristics. It provides analog out put which can be used to out put analog data to an x-y Recorder and to trace C-V curves. Also by interfacing with other instruments, it is possible to make a wide range of universal measurements. Figure 4.1.6 shows the I-V characteristic curve measured by Bantikassegn [45] using this and other devices.

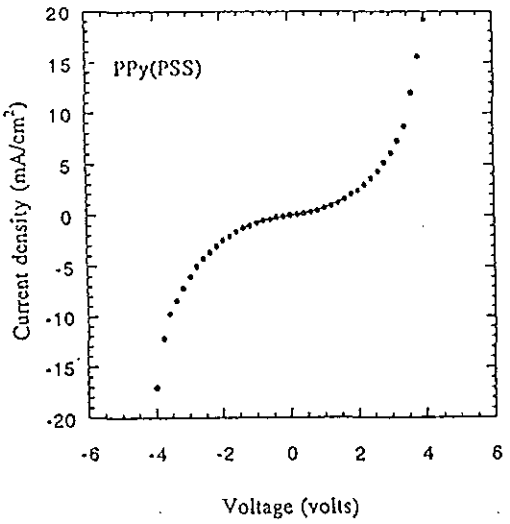

Fig. 4.1.6 The I-V measurement from reference [45].

4.2 Experimental Details

4.2.1 Sample Preparation

a) Absorption Spectrum Measurement.

Materials required for this purpose are: the spinner, PDOPT, chloroform, glass substrate and ethanol. The glass was cut to the required size and washed with ethanol. The chloroform solution of PDOPT with a concentration of 5mg/ml was prepared. The glass was placed on the chunk of the spinner and the solution of PDOPT was dropped on it. Then spinner was made to rotate at a speed of 600 rpm yielding thin and uniform film of PDOPT on glass ready for absorption measurement.

b) Impedance and I-V Measurements

Our working sample has a sandwich structure of Al/PDOPT/ITO on glass. Generally there are two techniques of preparing such sandwich devices:

1. The first and most common technique is the vacuum evaporation of Al at a very low pressure on the polymer spin coated on ITO-glass substrate. The thickness of the film of polymer can be controlled by its concentration and the rpm of the spinner.
2. The second method of preparation of a device with such a structure is known as Melt processing [47].

The group of M. Sundberg [47] used the melt processing technique to prepare their sample and they obtained a result which is the same as the result obtained in the first technique. For our case we followed the second way to prepare our sample. The PDOPT chloroform solution of concentration 5mg/ml was dropped on ITO/glass substrate. After about 10 min., the chloroform evaporated out leaving the PDOPT film on ITO-glass. Also the low work function metal (Al) was vacuum evaporated at a very low pressure on glass having a structure Al/glass. As Fig. 4.2.1 depicts, the Al/glass was put on PDOPT/ITO-glass and heated at about 50^0C and pressed until adhesion was achieved. The device was cooled down to room temperature before starting measurements. All metallic surfaces were cleaned by ethanol before processing. Processing and characterization was done at room temperature in laboratory atmosphere. Figure 4.2.1 depicts steps followed in sample preparation.

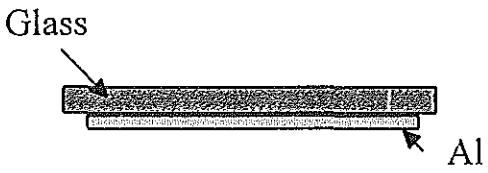

a) Al is evaporated on glass

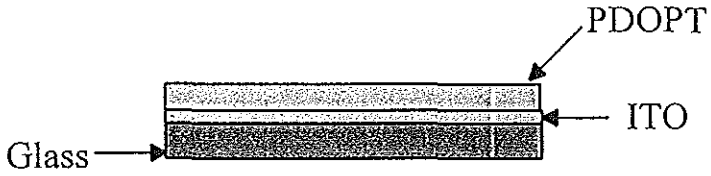

b) PDOPT is deposited on ITO-glass substrate

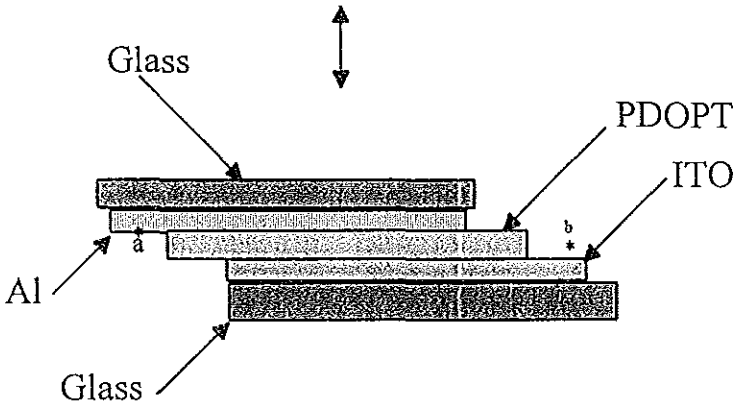

c) Al/PDOPT/ITO structure

Fig. 4.2.1 Schematics of Al/PDOPT/ITO sandwich structure prepared in the melt processing. Points a and b are the terminals of the device for electrical contacts.

4.2.2 Absorption Spectrum

The first task in this work is to identify whether or not PDOPT belongs to the class of semiconductors. This characteristic can be identified by measuring its energy gap from its absorption spectrum. To do so the chloroform solution of PDOPT with a concentration of 5mg/ml was spin coated on a glass substrate at 600 rpm yielding thin and uniform film. The thickness of this film is estimated to be about 300 nm. Then the thin film of PDOPT-glass was mounted on the sample holder of Perkin Elmer λ19 UV/Vis/NIR spectrophotometer.

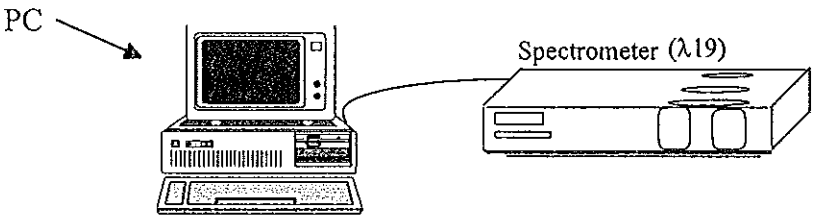

Fig. 4.2.2 Experimental set up for absorption measurement using λ19 Spectrophotometer.

Using a PC with UVCSS (Ultraviolet Computerized Spectroscopy Software) the absorption spectrum was obtained (see the result and discussion section). The threshold energy of absorption is assumed to correspond to the band gap energy.

4.2.3 The I-V Measurement

Figure 5.1.1 shows the current-voltage characteristics at room temperature in the dark of Al/PDOPT/ITO sandwich structure. The device prepared for the I-V measurement is a large area device with an effective contact area of about 0.49 cm^2. The I-V measurement was done for the biasing voltages running from -3.5V to +3.5V in steps of 0.1V.

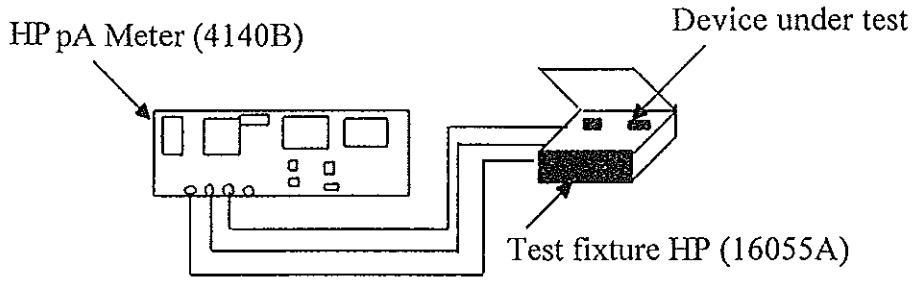

Fig. 4.2.3 Experimental set up for I-V measurement using HP pA meter (4140B).

4.2.4 Complex Impedance Analysis

We characterized the sandwich structure (Fig. 4.2.1) by measuring the complex impedance as a function of frequency and applied bias voltage. The complex impedance of the device was measured at frequencies from 50 kHz to 10 MHz for bias voltages ranging from -3V to +3V, in steps of 1V. Before the measurements were taken, the oscillation level was adjusted to be 0.01V. Zero offset adjustment of frequency was done at 100 kHz, 1 MHz and 10 MHz according to the instruction in the manual. The sample that we have produced for complex impedance analysis was a large area device with an effective contact area of about 0.78 cm^2. The Cole-Cole plot obtained for the device is displayed in the result and discussion section.

5. *Result and Discussion*

5.1 Absorption Spectrum of Neutral PDOPT

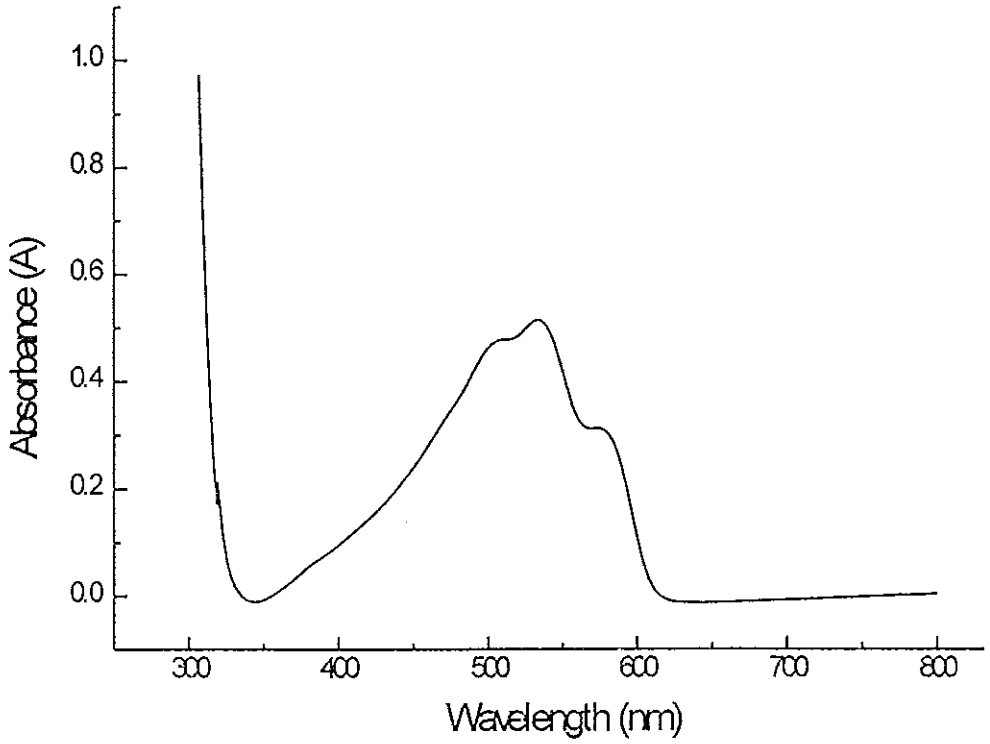

Fig. 5.1.1 Absorption spectrum of neutral PDOPT.

From the above curve the threshold energy of absorption is calculated from 612 nm to be about 2.02 eV. So in the classification of materials, those with an energy gap between 0.7 eV and 3 eV are regarded as semiconductors. Since the energy gap of PDOPT falls in this interval, we can conclude that PDOPT is a semiconducting polymer having $E_g = 2.02$ eV.

The two kinks that are seen are the vibronic states in the absorption spectrum. The vibronic feature is the result of high order and reduced inter-chain interactions in PDOPT [48]. The kink corresponding to higher energy is the energy absorbed when the vibration is out of phase and the one that corresponds to lower energy is when the vibration is in phase.

5.2 *The I-V Characteristic Curve.*

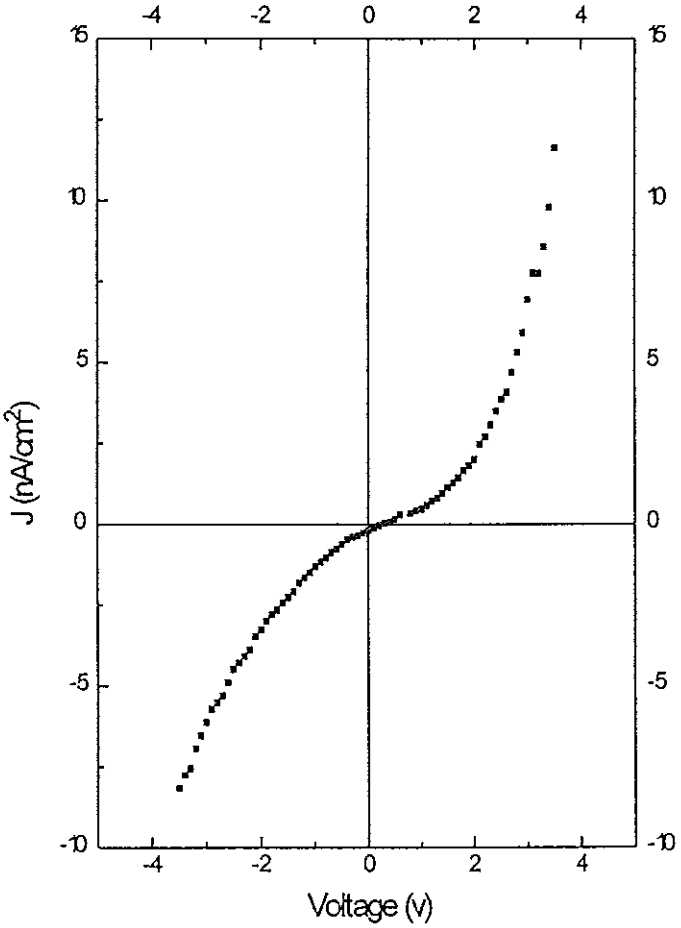

Fig. 5.2.1 The I-V characteristics of Al/PDOPT/ITO junction.

The characteristic curve obtained is symmetrical and non-ohmic. At lower values of the bias voltage, the junction became highly resistive and allows current passage in both directions for higher applied voltage. The I-V characteristic with the same feature was reported [37] for a structure of Al/PEDOT(PSS)/ITO, where PSS^- is large polymeric dopant anion.

5.3 *The Cole-Cole Plot*

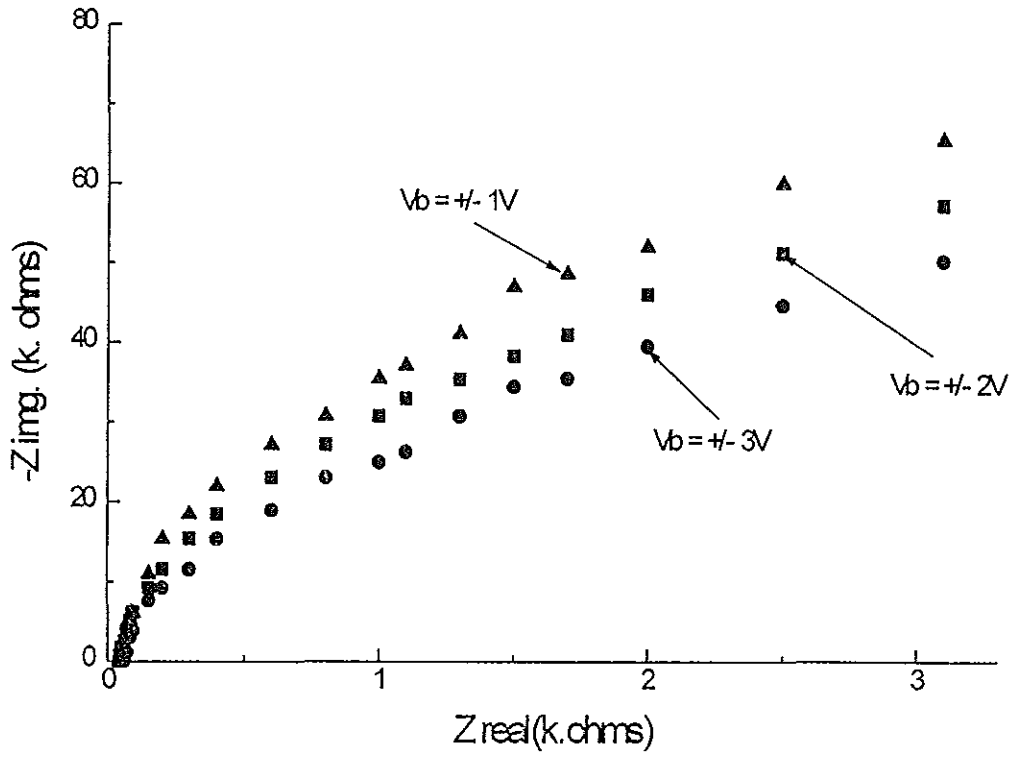

Fig. 5.3.1 Cole - Cole plot for Al/PDOPT/ITO structure at different bias voltages.

From Fig. 5.3.1, we observe that for all bias voltages, part of a single semicircle appeared. The diameter of these semicircles correspond to the real part of impedance. These semicircles are bias-voltage dependent. The diameters of these semicircles increase for small bias voltage (reverse or forward) and decrease for large bias voltage (reverse or forward). The data points are the measured co-ordinates representing the real and imaginary parts of the complex impedance which are characteristic of a given frequency. So we can model our sample (Al/PDOPT/ITO) by an equivalent electrical circuit given in Fig. 5.3.2.

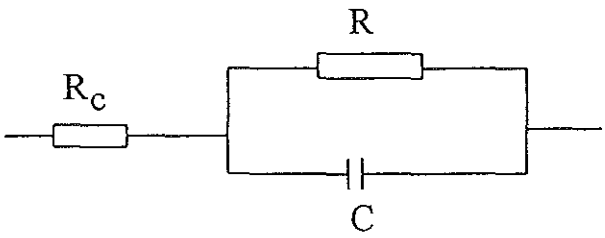

Fig. 5.3.2 An equivalent circuit for Al/PDOPT/ITO structure as modelled for the Cole-Cole plot of Fig. 5.3.1.

An ideal Cole-Cole plot of the complex impedance gives a semicircle with its center, the zero frequency and the 'infinite-frequency' intercepts on the Z_{real} axis. The zero-frequency of real impedance is obtained by extrapolation. The contact resistance, R_c is the distance from the origin to the intersection of the semicircle with the real axis of the impedance plot corresponding to the highest frequency. The distance between these intersection points (corresponding to the two extreme frequencies) on the Z_{real} axis is the real component of the impedance, R. The value of C is determined from the imaginary impedance equating it with $(\omega C)^{-1}$, i.e. $-Z_{img.} = (\omega C)^{-1}$. Knowledge of the frequency f ($\omega = 2\pi f$) and $-Z_{img.}$ gives the value of C for the corresponding bias voltage. The electrical parameters that are extracted from the Cole-Cole plot are listed in the table below. It has to be noted that the variation of the semicircles (their diameters) as a function of the applied voltage is consistent with the non-linear and symmetrical I-V curve.

Vb (V)	R (KΩ)	C (pF/cm^2)	R_c (Ω)
+/-3	7	0.44	50
+/-2	9	0.44	50
+/-1	10	0.45	50

Table 4.1 Electrical parameters extracted from the Cole-Cole plot of the Al/PDOPT/ITO device.

6. *Conclusion*

For the ITO/PDOPT/Al interface, the aluminium is easily oxidizable. The I-V characteristic curve and the complex impedance plot witnesses the absence of a Schottky barrier formation. A possible cause for a current limitation at the interface of Al/Polymer is the formation of an insulating region as a result of the reaction between the metal and the polymer. Other factors that contribute to the formation of this insulating film is that the π-bands of undoped polythiophenes and thiophene oligomers are strongly affected up on aluminium deposition. During the interface formation such reactions lead to the formation of sp^3 carbon site leading to the loss of conductance [7]. So this device, ITO/PDOPT/Al, may be considered as a metal-semiconductor device with no rectifying Schottky barrier formation at the Al/PDOPT interface. The small value of current may be due to the high bulk resistance of the polymer, as well as the probable formation of thick oxides of aluminium. The pictures of both the impedance spectroscopy and the I-V curve may be different if the aluminium were evaporated under high vacuum conditions. This needs further investigation.

7. *References*

[1] K.J. Saunders, *Organic Polymer Chemistry*, 2nd ed., Chapman & Hall Ltd. (1988).

[2] Alfred Rudin, *The Elements of Polymer Science and Engineering*, Academic Press Inc., London, (1982).

[3] L.R.G. Treloar, *Introduction to polymer science,* Wykeham Publications Ltd., London, (1970).

[4] S.L. Rosen, *Fundamental Principles of Polymeric Materials*, John Wiley & Sons, New York, (1982).

[5] A.G. Mac Diarmid, C.K. Chiang, C.R. Fincher, Jr., Y.W. Park, A.J. Heeger, H. Shirakawa, E.J. Louis and S.C. Gau, *Phys. Rev. Lett.,* **39** (1977) 1098.

[6] A.G. Mac Diarmid, C.K. Chiang, M.A Druy, S.C. Gau, A.J. Heeger, E.J. Louis, Y.W. Park, and H. Shirakawa, *J. Am. Chem. Soc.,* **100** (1978) 1013.

[7] W. Bantikassegn, PhD Dissertation, ISBN 91-7871-803-1, Linkoping University, Sweden, (1996).

[8] R.E. Hummel, *Electronic properties of materials*, 2nd ed., Springer-Vorlag, New York, (1993).

[9] Y. Teketel, PhD Dissertation, AAU, (1997).

[10] J.H. Burroughes, D.D.C Bradley, A.R. Brown, R.N. Marks, K. Mackay, R.H. Friend, P.L. Burns and A.B. Holmes, *Nature*, **347** (1990) 539.

[11] M. Berggren, O.Inganas, G. Gustafsson, J. Rasmusson, M.R. Andersson, T. Hjertberg, and O.Wennerstrom, *Nature,* **372** (1994) 444.

[12] D. Braun and A.J. Heeger, *Appl. Phy. Lett.*, **58** (1991) 1982.

[13] E. Smela, O. Inganas and I. Lundstrom, *Science*, **268** (1995) 1735.

[14] M.J. Yang, H.M. Sun, G. Casalbore -Miceli, N. Camaioni, C. -M. Mari, *Synthetic Metals*, **81** (1996) 65.

[15] P. Panayotatos, G. Bird, R. Sauers, A. Piechowski and S. Husain, *Solar Cells*, **21** (1987) 301.

[16] A.G. Mac Diarmid and A.J. Epstein, *Material Research Society Symp. Proc.*, **328** (1994) 33.

[17] M.G. Kantazidis, *Chemical and Engineering News*, December 3 (1990) 40

[18] R.M. Harrison and S.J. de Mora, *Introductory Chemistry for The Environmental Sciences*, 2nd ed., Cambridge University Press, Cambridge, (1996).

[19] S. Roth, *One dimensional Metals*, VCH Publishing Inc., New York, NY, (1995).

[20] Yu Lu, *Solitons and Polarons in Conducting Polymers*, World Scientific Publishing Co Pte Ltd., (1988).

[21] Y. Onodera, *Phys. Rev.*, B **30** (1984) 775.

[22] T. Ishiguro, H. Kaneko, Y. Nogami, H. Ishimoto, H. Nishiyama, J. Tsukamoto, A. Takahashi, M. Yamaura, T. Hagiwara and K. Sato, *Phys. Rev. Lett.*, **69** (1992) 660.

[23] Y.W Park, A.J. Heeger, M.A. Druy and A.G. Mac Diarmid, *J. Chem. Phys.*, **73** (1980) 946.

[24] C.M. Gould, D.M. Bates, H.M. Bozler, A.J. Heeger, M.A. Druy and A.G. Mac Diarmid, *Phys. Rev.*, B **23** (1981) 6820.

[25] E. Punkka, M.F. Rubner, J.D. Hettinger, J.S. Brooks and S.T. Hannans, *Phys. Rev.*, B **43** (1991) 9076.

[26] C.O. Yoon, M. Reghu, D. Moses and A.J. Heeger, *Phys. Rev.*, B **49** (1994) 10851.

[27] P. Sheng, E.K. Sichel and J.L. Gittleman, *Phys. Rev. Lett.*, **40** (1978) 1197.

[28] P. Sheng, *Phys. Rev.*, B **21** (1980) 2180.

[29] R.S. Kohlman, J. Joo, Y.Z. Wang, J.P. Pouget, H. Kaneko, T. Ishiguro and A.J. Epstein, *Phys. Rev. Lett.*, **74** (1995) 773.

[30] J. Joo, Z. Oblakowski, G. Du, J.P. Pouget, E.J. Oh, J.M. Wiesinger, Y. Min, A.G. Mac Diarmid and A.J. Epstein, *Phys. Rev.*, B **49** (1994) 2977.

[31] S.M. Sze, *Physics of semiconductor devices*, 2nd ed., John Wiley & Sons, New York, (1981).

[32] S. Wang, *Fundamentals of semiconductor theory and device physics*, Prentice Hall, New Jersey, (1998).

[33] D.A. Neamen, *Semiconductor physics and devices*, Richard D. Irwin, Boston, (1992).

[34] M.N. Rudden and J. Wilson, *Elements of solid state physics*, 2nd ed., John Wiley & Sons, Chichester, (1993).

[35] W. Bantikassegn, P. Dannetun, O. Inganas and W.R. Salaneck, *Thin Solid Films*, **224** (1993) 232.

[36] D.M. de Leeuw and E.J. Lous, Synthetic Metals, **65** (1994) 45.

[37] W. Bantikassegn and O. Inganas, *Thin Solid Films,* **293** (1997) 138.

[38] J.R. Macdonald, ed., *Impedance Spectroscopy, Emphasizing Solid Materials and Systems*, John Wiley & Sons, New York, (1987).

[39] HP 4192A LF Impedance Analyzer's Manual, Tokyo, (1986).

[40] K.S. Cole and R.H. Cole, J. Chem. Phys., 9 (1941) 341.

[41] Manual of the Spinner System, Model 4000 Photo Resist Coater.

[42] Manual of the Edwards Auto 306 Vacuum Depositor.

[43] Perkin Elmer λ19 spectrophotometer user's manual, Vol. 1, 2 and 3.

[44] W. Bantikassegn and O. Inganas, *Synthetic Metals,* **87** (1997) 5.

[45] W. Bantikassegn and O. Inganas, *J. Phys. D: Appl. Phys.*, **29** (1996) 2971.

[46] Manual of the pico Amper meter.

[47] M. Sundberg, G. Gustafsson and O. Inganas, *Appl. Phys. Lett.,* **57** (1990) 733.

[48] M.R. Andersson, M. Berggren, T. Olinga, T. Hjertberg, O. Inganas and O. Wennerstrom, *Synthetic Metals,* **85** (1997) 1383.